

1 **Effects of bark beetle attacks on forest snowpack and avalanche formation –**
2 **implications for protection forest management**

3 **Michaela Teich^{a,1}, Andrew D. Giunta^a, Pascal Hagenmuller^b, Peter Bebi^c,**
4 **Martin Schneebeli^c, and Michael J. Jenkins^a**

5 ^aDepartment of Wildland Resources, Utah State University, 5230 Old Main Hill, Logan, UT
6 84322-5230, USA

7 ^bUniv. Grenoble Alpes, Université de Toulouse, Météo-France, CNRS, CNRM, Centre d'Etudes
8 de la Neige, 1441 rue de la piscine, F-38400 Saint Martin d'Hères, France

9 ^cWSL Institute for Snow and Avalanche Research SLF, Flüelastrasse 11, CH-7260 Davos Dorf,
10 Switzerland

11 Corresponding author: Michaela Teich (michaela.teich@bfw.gv.at)

12 Declarations of interest: none

¹Present address: Department of Natural Hazards, Austrian Research Centre for Forests (BFW), Rennweg 1, 6020
Innsbruck, Austria

13 **Abstract**

14 Healthy dense forests growing in avalanche terrain reduce the likelihood of slab avalanche
15 release by inhibiting the formation of continuous snow layers and weaknesses in the snowpack.
16 Driven by climate change, trends towards more frequent and severe bark beetle disturbances
17 have already resulted in the death of millions of hectares of forest in North America and central
18 Europe affecting snowpack in mountain forests and potentially reducing their protective capacity
19 against avalanches. We examined the spatial variability in snow stratigraphy, i.e. the
20 characteristic layering of the snowpack, by repeatedly measuring vertical profiles of snow
21 penetration resistance with a digital snow micro penetrometer (SMP) along 10 and 20 m long
22 transects in a spruce beetle infested Engelmann spruce forest in Utah, USA. Three study plots
23 were selected characterizing different stages within a spruce beetle outbreak cycle: non-
24 infested/green, infested > 3 years ago/gray stage, and salvage-logged. A fourth plot was installed
25 in a non-forested meadow as the control. Based on our SMP measurements and a layer matching
26 algorithm, we quantified the spatial variability in snow stratigraphy, and tested which forest,
27 snow and/or meteorological conditions influenced differences between our plots using linear
28 mixed effects models. Our results showed that spatial variability in snow stratigraphy was best
29 explained by the percentage of canopy covering a transect ($R^2 = 0.71, p < 0.001$), and that only
30 14% of the variance was explained by the stage within the outbreak cycle. That is, differences
31 between green and gray stage stands did not depend much on the reduction in needle mass, but
32 spatial variability in snow stratigraphy increased significantly with increasing forest canopy
33 cover. At both study plots, a more heterogeneous snow stratigraphy developed, which translates
34 to disrupted and discontinuous snow layers and therefore reduced avalanche formation. We
35 attribute this to the small fine branches and twigs still present in the canopy of gray stage trees

36 influencing snow interception and unloading, and especially increasing canopy drip. In contrast,
37 salvage logging that reduced the canopy cover to ~25%, led to a spatially less variable and
38 similar snow stratigraphy as observed in the meadow. At these two study plots, a homogeneous
39 snow stratigraphy consisting of distinct vertical and continuous slope-parallel soft and hard snow
40 layers including weak layers had formed, which is generally more prone to avalanche release.
41 Our findings therefore emphasize advantages of leaving dead trees in place, especially in
42 protection forests where bark beetle populations have reached epidemic phases.

43

44 **Keywords:** snow stratigraphy; avalanche formation; protection forest; bark beetle; snow micro
45 penetrometer; SMP

46

47 **Highlights**

- 48 ▪ Snow penetration resistance was measured repeatedly below bark beetle killed trees
- 49 ▪ Variability in snow stratigraphy was quantified with a new layer matching algorithm
- 50 ▪ Spatial variability in snow stratigraphy is driven by percentage of canopy cover
- 51 ▪ Leaving dead trees in protection forests contributes to avalanche protection
- 52 ▪ Salvage logging can result in snow stratigraphy more prone to avalanche release

53 **1. Introduction**

54 Mountain forests growing in avalanche terrain serve an important role in avalanche
55 protection by reducing and disrupting the formation of continuous snow layers and weaknesses
56 in the snowpack that contribute to slab avalanches (Bebi et al., 2009; Schweizer et al., 2003). The
57 spatial deposition of snow and snow metamorphism determine snow stratigraphy, the
58 characteristic layering of the snowpack with varying properties, which develops over the course
59 of a winter (Pielmeier and Schneebeli, 2003). Forests modify snowpack properties through
60 interception of falling snow by tree crowns, the reduction of near-surface wind speeds, changes
61 to the energy balance beneath and around trees, and the direct support of the snowpack by stems,
62 remnant stumps and dead wood (Schneebeli and Bebi, 2004). Collectively these processes
63 promote a highly variable snow stratigraphy over space and time, which can inhibit avalanche
64 formation in forests (Bebi et al., 2009; Brang et al., 2006).

65 Native bark beetles (Coleoptera: Curculionidae: Scolytinae) are important disturbance agents
66 in forest ecosystems that naturally occur alongside their hosts (Jenkins et al., 2012, 2008; Raffa
67 et al., 2008). These insects infest weakened or stressed trees under endemic population phases
68 and, therefore, naturally alter forest ecosystems by killing live overstory trees, which creates
69 forest openings for other tree species and age classes to establish (Raffa et al., 2008; Veblen et
70 al., 1991). Under the right environmental and stand conditions as well as availability of suitable
71 host material, bark beetle populations can grow from an endemic to an epidemic phase, which
72 may overcome host resistance and initiate mass infestations that overwhelm healthy live trees
73 (Coulson, 1979). Recent bark beetle outbreaks in North America and central Europe have
74 reached unprecedented levels resulting in the death of millions of hectares of forest (Baier et al.,
75 2007; Black et al., 2013). Driven by climate variability and change, this trend towards more

76 frequent and severe disturbances is presumed to continue for the coming decades (Bentz et al.,
77 2010). Bark beetles are also expected to further colonize previously unsuitable habitats at higher
78 elevations and latitudes (Bentz et al., 2016; Logan et al., 2010; Seidl et al., 2009), which
79 profoundly affects snowpack in mountain forests (Edburg et al., 2012; Pugh and Small, 2012).

80 In the mountain forests of Europe, the European spruce bark beetle (*Ips typographus* L.) is
81 the most important biotic agent of disturbance infesting Norway spruce (*Picea abies* (L.) Karst.)
82 (Faccoli and Bernardinelli, 2014; Jönsson et al., 2009; Seidl et al., 2009). Likewise, the spruce
83 beetle (*Dendroctonus rufipennis* Kirby) is the most prevalent bark beetle species in high-
84 elevation Engelmann spruce (*Picea engelmannii* Parry ex Engelm.) dominated forests in western
85 North America (DeRose and Long, 2009; Hebertson and Jenkins, 2007; Veblen et al., 1991).
86 Both bark beetle species (hereafter collectively referred to as spruce bark beetles) have similar
87 impacts driving changes in community structure, composition, and function of spruce forests.
88 Unlike wind or logging disturbances where trees are removed from the vertical forest strata,
89 unmanaged beetle infested forests still retain stand structural integrity through standing dead tree
90 boles (Müller et al., 2008). Following spruce bark beetle induced tree mortality, a reduction in
91 canopy bulk density occurs (Jorgensen and Jenkins, 2011), as needles are shed from tree crowns
92 over a one to five year period (Page et al., 2014). The loss of needles reduces canopy interception
93 leading to enhanced subcanopy snow accumulation (Biederman et al., 2012; Pugh and Small,
94 2013; Winkler et al., 2014). Shifts from green-infested (current year's infestation) to phases
95 where foliar moisture content declines and needles fade from green to yellow (previous year's
96 infestation), to a gray phase that occurs when dead trees have dropped all their needles
97 (approximately three to five years post-infestation), gradually alter the energy balance at the
98 snow surface beneath canopies through increased light transmission and wind speeds (Boon,

99 2009; Perrot et al., 2014). This also reduces snow surface albedo through increased litter
100 accumulation on the snow surface (Winkler et al., 2010). These changes influence subcanopy
101 snow stratigraphy significantly by altering snow (re-)distribution and metamorphism with
102 uncertain consequences for the avalanche hazard. That is, the reduction in canopy bulk density
103 may promote the formation of more homogeneous and continuous snow layering and weaknesses
104 in the snowpack that are linked to slab avalanche formation (Schweizer et al., 2003). For
105 example, the occurrence of deciduous tree species was found to be one key forest structural
106 parameter that influences avalanche formation in forested areas (Schneebeili and Meyer-Grass,
107 1993). Bebi et al. (2009) found that the presence of European larch (*Larix decidua* Mill.) is an
108 important factor that increases the probability of avalanche release from spruce and larch
109 dominated subalpine forests on steep slopes (slope angle $>30^\circ$), in particular if they have a crown
110 cover density between 30 and 50%. Moreover, the minimum gap widths required for avalanche
111 formation in such subalpine forests is only 5-10 m compared to 20 m for coniferous forests with
112 a crown cover density of 60% (Schneebeili and Bebi, 2004). Spruce bark beetle-induced tree
113 mortality may therefore create potential avalanche release areas where the forest previously
114 protected settlements and infrastructure against avalanches (Bebi et al., 2017; Teich et al., 2016).

115 Managing protection forests for stability, resilience and sustainability is a long-term
116 investment for mitigating the avalanche hazard (Motta and Haudemand, 2000). In the European
117 Alps, avalanche protection forests primarily consist of Norway spruce and are therefore
118 susceptible to frequent epidemic and severe European spruce bark beetle outbreaks as predicted
119 for the coming decades (Seidl et al., 2009). Current management strategies include salvage
120 logging to remove infested trees through costly helicopter operations with the goal to reduce the
121 expansion of ongoing spruce bark beetle outbreaks and the potential decline in forest's protective

122 effects against avalanches (Brang, 2001). However, little research has been conducted into
123 whether or not and over what timespan infested spruce forests may still provide protection
124 against avalanche release (Bebi et al., 2017), and only few studies have examined the
125 stratigraphy of subcanopy snowpack in general (Fiebiger, 1978; Imbeck, 1983; Molotch et al.,
126 2016; Perrot et al., 2014; Sturm, 1992; Zingg, 1958), despite its considerable contribution to
127 forest avalanche formation (Teich et al., 2013). To our knowledge, no study to date has
128 investigated the effects of spruce bark beetle infestations on the evolution of subcanopy snow
129 stratigraphy linked to avalanche protection by forests.

130 Snowpack observations in forested terrain are rare, and typically describe layering and
131 related physical and mechanical properties by point observations with snow pit profiles
132 (Fiebiger, 1978; Imbeck, 1983; Imbeck and Ott, 1987; Zingg, 1958). Such point observations
133 emphasize and illustrate the heterogeneous stratigraphy of subcanopy snowpack, but are not able
134 to adequately describe spatially distributed effects of forests on the evolution of snow
135 stratigraphy throughout the snow season. Furthermore, manual snow pit profiles disturb the
136 snowpack such that repeat measurements are not possible, and are highly dependent on observer
137 skills introducing uncertainty and potential bias, if the snow pit profile is mischaracterized. In
138 contrast to time- and labor-intensive manual snow pit profiles, the SnowMicroPen (SMP) is a
139 portable and minimally invasive digital penetrometer, which quickly measures snow penetration
140 resistance along a vertical profile (Johnson and Schneebeli, 1999; Schneebeli and Johnson,
141 1998). Therefore, snow layering can be identified from SMP penetration resistance profiles
142 enabling an unambiguous investigation of snow stratigraphy and if several adjacent SMP
143 measurements are taken, its spatial variability. Due to that spatial variability in snow stratigraphy,
144 continuous snow layers are not necessarily positioned at the same depth in adjacent

145 measurements. To quantify spatial variability it is therefore necessary to track common layers
146 between different SMP penetration resistance profiles (e.g. Kronholm et al., 2004). This tracking
147 was generally performed manually, which limits the amount of SMP penetration resistance
148 profiles to be processed and the number of snow layers to be compared (e.g. Kronholm et al.,
149 2004; Sturm and Benson, 2004). By automatically tracking distinct snow layers with a recently
150 developed matching method, vertical and slope-parallel variabilities in snow stratigraphy
151 observed by several spatially distributed SMP measurements, can now be disentangled and
152 quantified (Hagenmuller and Pilloix, 2016). This quantification can be used to infer, if a snow
153 stratigraphy observed at one site might be more (homogeneous snow stratigraphy) or less
154 (heterogeneous snow stratigraphy) prone to avalanche release. We define a homogeneous snow
155 stratigraphy as continuous slope-parallel snow layering with a distinct vertical heterogeneity. In
156 contrast, a heterogeneous snow stratigraphy is characterized by less distinct vertical snow
157 layering that discontinue parallel to a slope.

158 We used the SMP to repeatedly examine the snowpack under tree canopies of spruce beetle
159 infested Engelmann spruce forest stands in the Uinta Mountains in Utah, USA, over two winter
160 seasons. We then applied the described matching algorithm to our dataset to quantify the
161 observed spatiotemporal variability in snow stratigraphy.

162 We hypothesize that:

- 163 1) Associated with the decrease in live canopy, spatial variability in snow stratigraphy is
164 gradually decreasing from a more heterogeneous snowpack to a more homogeneous
165 snowpack (i.e., increasing distinct vertical and continuous slope-parallel snow layering)
166 from green and green-infested to gray stage to salvage-logged spruce forest stands.

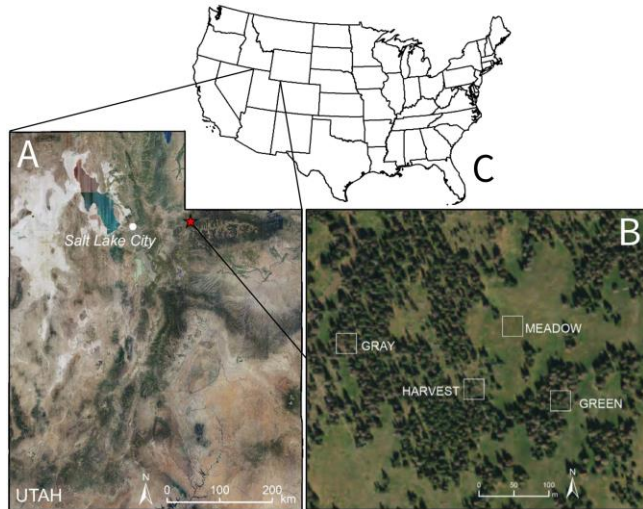
- 167 2) Forest canopy condition (i.e., green and green-infested vs. gray stage vs. salvage logged
168 forest stands vs. no canopy), in combination with typical snow and meteorological
169 patterns, is the main driver for changes to the spatial variability in snow stratigraphy.
- 170 3) Surface roughness in terms of the amount and height of downed woody debris is linked to
171 a greater heterogeneity in the spatial variability of snow stratigraphy.

172 We test and discuss our hypotheses by linking the quantified spatiotemporal variability in
173 snow stratigraphy to forest, snow and meteorological conditions. Guided by our small-scale but
174 highly detailed observations, we develop a conceptual framework describing the effects of
175 subalpine spruce forests on snow stratigraphy following spruce bark beetle outbreaks years to
176 decades after infestation, and discuss implications for avalanche protection forest management.
177 Developing appropriate mitigation and adaptation measures is important throughout subalpine
178 spruce forests across Europe where infestations by European spruce bark beetle have been
179 increasing (Faccoli, 2009; Grodzki, 2007; Jonášová and Prach, 2008; Seidl et al., 2014), and
180 particularly in densely populated mountain regions where protection forest management is
181 critical for safeguarding property, lives, and infrastructure (Dorren et al., 2004; Olschewski et al.,
182 2012).

183 **2. Methods**

184 **2.1 Study site and plot descriptions**

185 Our study site was located in an Engelmann spruce-subalpine fir (*Abies lasiocarpa* (Hooker)
186 Nuttall) forest at an elevation of approximately 2900 m in the Uinta Mountains in Utah, USA
187 (40.854655N 110.9568W; Fig. 1).



188

189 **Fig. 1.** Study site (A), and study plot (B) locations including one green stand (GREEN), one gray stage
 190 stand (GRAY), one salvage-logged stand (HARVEST), and one meadow area (MEADOW) in the Uinta
 191 Mountains in Utah, USA (C). Imagery from National Agricultural Imagery Program (USDA Farm Service
 192 Agency, 2014).

193 Four study plots were selected in October 2014 in close proximity to each other (< 350 m) to
 194 minimize meteorological and topographical differences between study plots while characterizing
 195 different stages during a spruce beetle outbreak cycle (Table 1, Figs. 1 and 2).

196

197 **Table 1**

198 Topography of four selected study plots at the study site in the Uinta Mountains in Utah, USA (Fig. 1).

Topography	Study plot*			
	GREEN	GRAY	HARVEST	MEADOW
Elevation (m)	2909	2901	2909	2896
Slope (°)	5	5-10	10	10
Aspect	N-NE	N	NW	N

199 GREEN = green stand; GRAY = gray stage stand; HARVEST = salvage-logged stand; MEADOW = non-
 200 forested meadow area

201 *Each study plot was approximately 200 m² in size

202 We selected four plots that were (1) non-infested by *Dendroctonus rufipennis* (hereafter
203 referred to as GREEN), (2) infested > 3 years prior to the study (GRAY), (3) salvage logged
204 (HARVEST), and (4) an open meadow plot as a control (MEADOW; Fig. 2).

205



206

207 **Fig. 2.** Stand conditions of study plots in summer 2015 (A, B, C) and winter 2016 (D): A) GREEN, B)
208 GRAY, C) HARVEST, and D) MEADOW (see Fig. 1 for locations). Photos: Michaela Teich

209 Salvage logging is a post-disturbance forest management strategy designed to recuperate
210 wood product value, reduce hazardous fuels, and to enhance regeneration (Lindenmayer and
211 Noss, 2006). The HARVEST plot was salvage logged in the fall of 2013 (USFS personal
212 communication) where dead overstory spruce were removed and live overstory and understory
213 trees were retained with dbh (diameter at breast height; measured at 1.37 m above ground) < 15
214 cm. This size class of trees is less prone to spruce bark beetle attack (Fettig et al., 2007). Logging

215 activities increased the surface roughness over this plot through the spread of residual logging
216 slash with effective woody debris heights found to be up to 0.95 m (Fig. 2C). A non-forested plot
217 was installed and delineated by a roped boundary to prevent anthropogenic disturbance in an
218 open MEADOW as the control, representing a total removal of forest canopy cover (Fig. 2D).
219 During plot establishment, standard forest mensuration measurements of forest structure
220 including stem density, tree height, dbh, crown diameter, canopy base height, percentage of
221 canopy cover, and percentage of live canopy were collected in each plot.

222 After plot selection and beginning with winter snowpack data collection, few trees (< 5) in
223 the GREEN plot showed signs of current year's spruce beetle infestation, i.e. reddish-brown frass
224 had accumulated at the base of trees, and beetle entrance holes were visible, but needles were
225 still green and had yet to fade. During the winter of 2014/2015 (hereafter referred to as winter of
226 2015), the infested trees were partially debarked by woodpeckers leaving layers of bark flakes on
227 the snow surface around the boles of trees, which were subsequently buried throughout the snow
228 season. Needles of infested trees started to turn yellowish-green and needle release began during
229 the winter of 2015/2016 (hereafter referred to as winter of 2016) increasing the litter content on
230 the snow surface and at snow layer boundaries. As we revisited the GREEN plot in July 2016
231 (after winter field campaigns were completed), almost all trees had become infested, and 5-10%
232 of trees had begun to lose the majority of their needles indicating that they were dead.

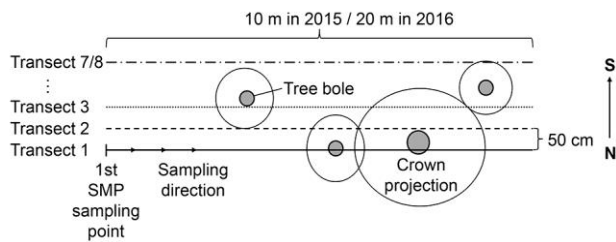
233 Trees in the GRAY plot were attacked in 2011 and had already dropped needles at the time of
234 study plot establishment leaving the upper crowns exposed with only twigs and small branches
235 still attached (Fig. 2). Gray trees were interspersed with few green-infested trees which
236 consistently dropped needles onto the snow surface throughout both winters.

237 **2.2 Field measurements**

238 The SnowMicroPen (SMP) is a digital snow penetrometer that records penetration resistance
239 with a constant penetration speed of 20 mm s⁻¹ every 4 μm to a depth of 1.2 m (Schneebeli and
240 Johnson, 1998). The SMP measures the penetration resistance in a range from 0.01 N for soft
241 low density snow up to 41 N (which was manually set as overload limit to prevent sensor
242 damage) for dense hard snow. The obtained depth-resistance signals (further referred to as SMP
243 profiles) can therefore be interpreted as snow hardness measurements, which are used in practice
244 and research as indicators for snow mechanical properties (Fierz et al., 2009; Marshall and
245 Johnson, 2009), and thus snowpack stability (Reuter et al., 2015).

246 We used the SMP to examine the snow stratigraphy and to monitor the evolution of the
247 snowpack in our four study plots from mid-January to mid-April of 2015 and 2016 for a total of
248 15 winter field campaigns (Table A1). During the first campaign of each sampling season, we
249 defined and marked start and endpoints of the initial transect (Transect 1) in each of the four
250 plots, which served as reference for all following field campaigns (Fig. 3; Table A1).

251



252

253 **Fig. 3.** Schematic of sampling design. SnowMicroPen (SMP) measurements were taken in an east to west
254 direction at 0.3 m intervals in winter of 2015 and increased to every 0.5 m in winter of 2016.

255 In 2015 transects were 10 m in length and adapted to 20 m in length in 2016, and in both
256 years oriented in an east-west direction. We recorded SMP measurements along the entire length

257 of each transect at 0.3 m intervals in 2015 and in 0.5 m increments in 2016 resulting in a
258 maximum of 34 (2015) and 41 (2016) sampling points per study plot and sampling date. We
259 omitted sampling points, if their location coincided with a tree bole, and moved on to the next
260 sampling point along a transect. In addition to SMP recordings, we measured snow depth with a
261 300 cm graduated avalanche probe and canopy cover by using a GRS Densitometer (Geographic
262 Resource Solutions; Forestry Suppliers, Jackson, MS) at each SMP sampling point. The
263 densitometer was used by two independent observers to determine whether the reading was open
264 sky (recorded as 0) or if canopy was present (recorded as 1). The percentage of canopy cover
265 was calculated for each transect from the number of canopy readings (record 1) divided by the
266 total number of readings per transect. The mean height of the snowpack (HS) was calculated
267 from our snow depth measurements for each transect and sampling date.

268 Each week during 2015, and every other week during 2016, transect start and endpoints were
269 moved 0.5 m south from the previous point and measurements were repeated along each transect.
270 This 0.5 m offset was sufficient to avoid any potential disturbances of snow layers along the
271 current sampling transect that may have resulted from previous SMP measurements and/or
272 footprints. In total, we sampled eight times throughout winter 2015 spanning a period of nine
273 weeks and seven times in 2016 over a 14-week period.

274 During each field campaign, a snow pit profile was excavated in the MEADOW plot. Each
275 pit boundary was marked by bamboo poles so previous pit locations could be avoided during
276 subsequent site visits. The International Classification for Seasonal Snow on the Ground (Fierz et
277 al., 2009) was used to manually assess and classify layering, grain shape, grain size, and hand
278 hardness.

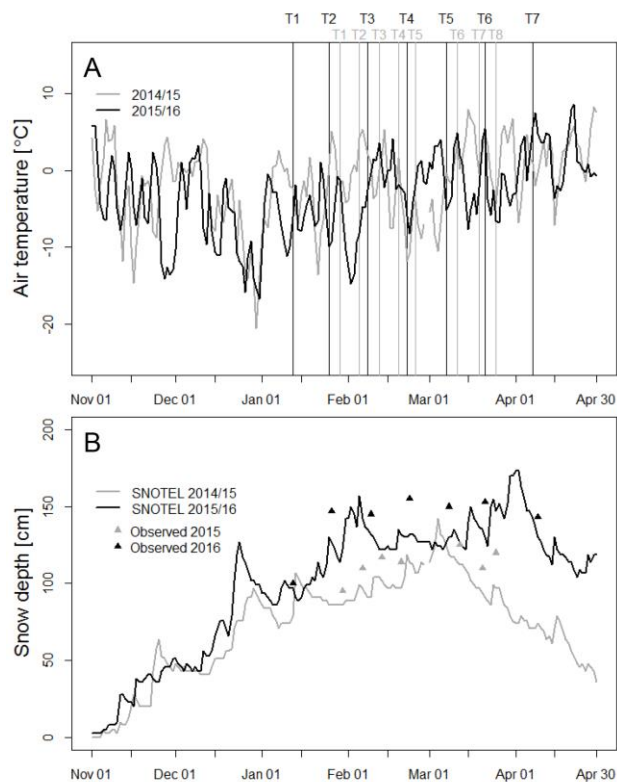
279 Surface roughness in terms of downed woody material present at GREEN, GRAY, and
280 HARVEST plots was measured in August 2015 and June 2016. Ten and 20 m long transects
281 matching the exact location of the snowpack measurement transects were established. Along
282 each transect the height and width of underlying down woody debris pieces were measured using
283 a standard meter tape and counted along every other transect for each fuel diameter size class (1
284 hour fuels ≤ 0.6 cm, 0.6 cm < 10 hour fuels ≤ 2.5 cm, 2.5 cm < 100 hour fuels ≤ 7.6 cm, 1000
285 hour fuels > 7.6 cm) following the method described in Brown (1974). We used these
286 measurements to calculate mean and maximum heights of debris > 7.6 cm in diameter (coarse
287 woody debris, CWD), and the volume per ha of downed woody material for each fuel diameter
288 class (see Brown, 1974), to retrieve a standardized measure describing the surface roughness
289 found in our three forested study plots.

290 **2.3 Climate conditions and meteorological data**

291 The climate in the study area is typical of a continental subalpine site in the western USA,
292 having a dry summer/wet winter pattern (Shaw and Long, 2007), with the majority of
293 precipitation falling as snow during the winter months November through April (Gillies et al.,
294 2012; Munroe, 2003). Meteorological data of the study area are measured by Natural Resources
295 Conservation Service (NRCS) SNOWpack TELemetry (SNOTEL) stations. The closest SNOTEL
296 site is Chalk Creek #1 (ID392) and is located approximately 150 m lower at an elevation of 2741
297 m and 8.2 km west of the study site. Daily data for snow depth and average air temperature were
298 obtained for both winters (starting November 1) from the SNOTEL network via the NRCS
299 website (www.wcc.nrcs.usda.gov/snow/; [accessed on 2 August 2017]) describing winter
300 conditions over the study period (Fig. 4). During both winters, a permanent snow stake was

301 installed at the MEADOW plot and readings were recorded when approaching the plot during
302 each winter field campaign (Fig. 4).

303



304

305 **Fig. 4.** Daily average air temperature (A), and total snow depth measured at SNOTEL site Chalk Creek #1
306 (ID392), and snow depths observed with a snow stake permanently installed at the MEADOW plot (B) in
307 winters of 2015 and 2016. Vertical lines indicate first day of sampling transects (T) 1-8 in 2015 and
308 T1-7 in 2016; the majority of measurements were taken on two consecutive days (Table A1).

309 To characterize the general weather pattern prior to each sampling date, which, in
310 combination with the forest cover, may have influenced the snow stratigraphy observed at our
311 four plots, we used daily values for average temperatures and accumulated precipitation from the
312 SNOTEL site Chalk Creek #1 and calculated a set of variables known to be associated with
313 avalanche release from forests (Teich et al., 2012, 2013; Table 2). Precipitation as well as

314 temperature variables were calculated for one to three day periods prior to our sampling dates
 315 since, if driven by temperature gradient metamorphism, complete turnover of snow crystals
 316 appears within a rather short time where little if any of the original grain remains after two to
 317 three days (Pinzer et al., 2012).

318

319 **Table 2**

320 Variables on meteorological conditions present prior to each winter field campaign calculated based on
 321 daily values for average air temperature and accumulated precipitation obtained from SNOTEL site Chalk
 322 Creek #1 (ID392). All data was screened manually for outliers and obvious instrument errors.

Variable	Symbol
Average air temperature 1 day prior to measurements (°C)	T _{a1}
Average air temperature within a 3-day period prior to measurements (°C)	T _{a3}
Average air temperature difference between 1 and 3 days prior to measurements (°C)	ΔT _{a3}
Accumulated precipitation 1 day prior to measurements (mm)	N1
Accumulated precipitation 1 to 3 days prior to measurements (mm)	N3

323

324 **2.4 SMP profile processing and similarity metrics calculations**

325 Prior to processing, all SMP recordings were checked for signal errors and quality according
 326 to the classification scheme of Pielmeier and Marshall (2009). Only profiles which were
 327 classified as "C1" (no error), and "C2" signals (trend or offset in absolute SMP penetration
 328 resistance) with a negligible linear drift in the air signal were retained. Air/snow and
 329 snow/ground interfaces were determined manually and cut-off automatically through profile
 330 processing from the initial SMP profile leaving only the signal recorded within each snowpack.

331 Profiles were automatically adjusted for offsets. Hereafter, we interpret the snow penetration
332 resistance measured by the SMP as a measure for snow hardness.

333 We further processed SMP profiles collected along each transect at each sampling date using
334 the matching algorithm developed by Hagenmuller and Pilloix (2016). Due to variations in
335 internal layer thicknesses observed in a set of measurements, layers at the same depth are not
336 necessarily at the same position in the stratigraphic sequence, which creates an apparent spatial
337 variability in stratigraphic features. To account for these stratigraphic mismatches, Hagenmuller
338 and Pilloix (2016) developed a method to automatically adjust layer thicknesses to minimize the
339 difference between adjacent SMP profiles. This provides us qualitative and quantitative measures
340 to compare differences in snow stratigraphy observed throughout the two winters at our four
341 study plots and to test, which forest, snow and/or meteorological conditions influence the spatial
342 and temporal variability in the layering of subcanopy snowpack.

343 The algorithm consists of three steps:

344 1. SMP profile transformation and re-sampling on a regular grid:

345 Each SMP profile is first re-sampled onto a one-dimensional regular depth grid h spanning 0
346 to 120 cm (maximum SMP measurement depth) with a constant 0.1 cm vertical step Δh defining
347 the resolution of the re-sampled profile (σ, h) by preserving thin snowpack features after re-
348 sampling. The transformation procedure T modifies the depth h by stretching or thinning the
349 thickness l of the recorded layers j by a constant factor α_j , i.e., the new thickness of layer j is $\alpha_j \times$
350 Δl . We restricted the transformation to stretch or thin the layer thickness by less than a factor of
351 two, i.e., α_j , in $[0.5, 2]$. The transformed depth points h_T of the hardness measurements σ are then
352 derived from the new layer thicknesses, but h_T do not necessarily lie onto the regular grid points

353 h . The transformed profile (σ, h_T) is thus linearly interpolated on the regular depth grid to obtain
354 the final profile (σ_T, h) .

355 2. Similarity metrics:

356 To quantify how similar individual SMP profiles are, we define two metrics: a) a distance D
357 between one profile and a reference profile, and b) the intra-set variability V of a set of multiple
358 profiles.

359 a) The distance D between two profiles (σ, h) and (σ_{ref}, h) , which are re-sampled on the
360 same depth grid h is defined as the mean square difference of the hardness in a log-
361 scale ensuring that hardness differences of crusts are as important as differences of
362 soft (including weak) layers.

363 b) The intra-set variability V is defined as the standard deviation of the hardness
364 logarithm for a given height between different profiles, which is then averaged over
365 the depth of the whole profile. V therefore quantifies how different several profiles
366 are from each other without appointing one of them as the reference.

367 3. Optimization and quantification of spatial variability:

368 To quantify the similarity between two SMP profiles accounting for potential depth shifts, we
369 computed the transformation T that minimizes the distance D between profile (σ_T, h) , that is, the
370 profile (σ, h) transformed by T , and profile (σ_{ref}, h) . The resulting minimal distance D_{min} is a
371 measure of the similarity between the two profiles (i.e., if $D_{min} = 0$, then the two profiles are
372 considered the same; if $D_{min} = +\infty$, then the two profiles are completely different) neglecting
373 impacts of layer thickness variations in the range [-50%, +100%]. Hereafter, we denote D_{min} by
374 D .

375 We computed a pairwise distance matrix for our data set by matching and comparing each
376 SMP profile collected along a transect with every other SMP profile recorded along that transect.
377 The intra-set median distance was then calculated as the median D of all SMP profile pairs.

378 To quantify the similarity between more than two SMP profiles accounting for potential
379 depth shifts, we computed the set of transformations $\{T\}$ that minimized the intra-set variability
380 V between all profiles transformed by $\{T\}$. This complex optimization problem was heuristically
381 solved by iteratively matching each profile to the mean profile of the set (evolving with
382 iterations) as proposed by Petitjean et al. (2011). The resulting minimal intra-set variability V_{min}
383 provides a quantitative measure of the variability of SMP profiles collected at a given site and
384 time (i.e., if $V_{min} = 0$, then all profiles are considered the same; if $V_{min} = +\infty$, then the profiles are
385 completely different) neglecting impacts of layer thickness variations in the range [-50%,
386 +100%]. The mean profile of the transformed profiles also provides one representative profile for
387 the SMP profile set. Hereafter, we denote V_{min} by V . For further details about the matching and
388 optimization procedure see Hagenmuller and Pilloix (2016).

389 **2.5 Data analysis**

390 First, repeated measures ANOVA ($\alpha = 0.05$) and paired-samples t-tests were conducted to
391 compare V (intra-set variability), which we calculated for each sampled transect and year as a
392 measure to quantify the combined vertical and slope-parallel variability in snow stratigraphy (see
393 section 2.4), between our four study plots GREEN, GRAY, HARVEST and MEADOW.

394 We then used linear mixed effects models (LMMs; Zuur et al., 2009) to characterize the
395 relationships between forest, snow and meteorological variables as potential drivers for
396 variability in snow stratigraphy, and the response variable V . LMMs extend traditional linear
397 models by including a combination of fixed and random effects as predictor variables explicitly

398 allowing to model non-independent observations and are therefore suitable for running repeated
 399 measures analyses (Zuur et al., 2009). Modeling random effects that typically represent some
 400 grouping variable supports correct inference about fixed effects and allows the estimation of
 401 variance in the response variable within and among these groups (Harrison et al., 2018). We used
 402 LMMs since we took repeated SMP measurements grouped by our four study plots every week
 403 (in winter of 2015) and every other week (in winter of 2016) in a snowpack that developed over
 404 the season and measurements are therefore not independent. Using LMMs allowed us to estimate
 405 the effects of explanatory variables (fixed effects) on V while also estimating and controlling for
 406 effects on V of the selected study plots (PLOT) and differences in winter conditions between
 407 2015 and 2016 (YEAR; random effects) that were not accounted for with fixed effect terms.

408 Tested drivers for variability in snow stratigraphy were percentage of canopy cover, CWD
 409 mean and maximum heights (forest variables), a set of five meteorological variables (see Table
 410 2), and mean height of the snowpack (snow variable). All these drivers were treated as fixed
 411 effects and “PLOT” and “YEAR” (for models that included both winters’ data) as random effects
 412 during model development and selection, which was guided by our global model:

$$413 \quad V = f \{ \text{CANOPY} + \text{DEBRIS}_{\text{mean}} + \text{DEBRIS}_{\text{max}} + T_a1 + T_a3 + \Delta T_a3 + N1 + N3 + \text{HS} \\ 414 \quad \quad \quad + (1|\text{PLOT}) + (1|\text{YEAR}) \}$$

415 where V = intra-set variability; CANOPY = percentage of canopy cover per transect;
 416 DEBRIS_{mean} = CWD mean height per transect; DEBRIS_{max} = CWD maximum height per
 417 transect; see Table 2 for descriptions of T_a1 , T_a3 , ΔT_a3 , $N1$, $N3$; HS = mean height of the
 418 snowpack per transect; PLOT = four study plot categories GREEN, GRAY, HARVEST and
 419 MEADOW; YEAR = winter the transect was sampled, 2015 or 2016; the parentheses indicate

420 the term is a random effect (*re*), all other terms are fixed effects; (1 | *re*) indicates that the
421 intercept was allowed to vary randomly.

422 To analyze and test for differences between winters 2015 and 2016, we fit a model for each
423 year separately and one for both years combined. To derive the “best-fit” models, we followed a
424 four-step procedure: 1) We determined the optimal random effects structure for the model
425 including data of both years and selected amongst three LMMs (fit with restricted maximum
426 likelihood) with possible combinations of random effects “PLOT” and “YEAR”, but with no
427 fixed effect term. 2) We used the function “dredge” implemented in the R package MuMIn
428 (Barton, 2018) to automatically fit and rank LMMs with all possible combinations of fixed effect
429 terms (all forest, snow and meteorological variables) and the random effect structure selected in
430 step one (fit with maximum likelihood). 3) Based on the results of steps one and two, and our
431 hypotheses, we selected the variables and their two-way interactions to be included in the models
432 to be further tested (fitted with maximum likelihood). 4) We fit the models selected for each year
433 and the one combining both winters with restricted maximum likelihood and considered these
434 models to be our final “best-fit” models (Zuur et al., 2009).

435 Akaike’s information criteria (Akaike, 1973) with small sample bias adjustment (AICc;
436 Hurvich and Tsai, 1989) was used to determine the most parsimonious combination of fixed
437 effect terms to select amongst models. For our best-fit models, we assessed the significance of
438 the fixed-effects model coefficients using *F*-tests, and calculated marginal R^2 as the proportion of
439 variance in the response variable explained by the fixed effect explanatory variables, and
440 conditional R^2 , which can be interpreted as the variance explained by both fixed and random
441 effects terms, i.e. by the entire model (Nakagawa and Schielzeth, 2013; Xu, 2003). All models
442 were fit in R version 3.5.0 using the lme4 package (Bates et al., 2015; R Core Team, 2018). The

443 R package MuMIn was used to support model selection, and test statistics were calculated with
444 functions implemented in MuMIn or the R package car (Barton, 2018; Fox and Weisberg, 2011).
445 We verified that the model residuals were normally distributed to validate using linear mixed
446 effects models rather than generalized linear mixed effects models.

447 **3. Results**

448 **3.1 Forest characteristics**

449 Forest stand structure is similar between GREEN and GRAY study plots in terms of mean
450 dbh, tree height, and crown diameter (Table 3). The GREEN plot was found to have a higher
451 mean stem density and mean basal area compared to GRAY and HARVEST plots. Overall
452 percentage of canopy cover was much higher in GREEN (85%) and GRAY (80%) plots
453 compared to the HARVEST plot (27%). The percentage of live canopy decreased over the course
454 of the entire study in GREEN and GRAY plots. In the GREEN plot initial infestation occurred in
455 2014, yet trees still retained the majority of live canopy during 2015 and 2016 winter campaigns.
456 Spruce beetle infestation reached its highest level in summer 2016 where a reduction to 47% live
457 canopy was estimated in June after winter field campaigns were completed. However, percentage
458 of live canopy was always higher in the GREEN plot compared to the GRAY plot. The initial
459 percent of live canopy cover found in the GRAY plot were attributed to interspersed subalpine
460 firs and residual spruce saplings that were not infested by spruce beetles, and decreased only
461 slightly over the course of the study to 34%.

462 Surface roughness associated with down woody debris is expected to influence snow
463 stratigraphy. We found loading of fine woody debris (FWD) with diameters < 7.6 cm (1, 10 and
464 100 hour fuels) was highest in the HARVEST plot associated with residual slash following
465 harvesting (Table 3). The HARVEST plot also had a higher mean CWD load (1000 hour fuels)

466 compared to GREEN and GRAY plots, and was found to have the highest maximum CWD fuel
 467 heights whereas the greatest overall mean CWD height was found in the GRAY plot.

468

469 **Table 3**

470 Stand characteristics (measured during plot establishments in October 2014) and fuel load characteristics
 471 (collected in August 2015 and June 2016) for forested study plots GREEN, GRAY, and HARVEST in the
 472 Uinta Mountains in Utah, USA.

	GREEN		GRAY		HARVEST	
	<i>M</i>	<i>SD</i>	<i>M</i>	<i>SD</i>	<i>M</i>	<i>SD</i>
dbh (cm)	28	13	30	10	18	3
Height (m)	17.5	5.9	17.6	5.0	14.4	3.7
Canopy base height (m)	6.1	4.1	4.6	2.6	5.5	2.4
Crown diameter (cm)	370	166	381	190	267	56
CWD mean height (cm)	18	20	21	12	17	14
Density (stems ha ⁻¹)	1127	-	676	-	526	-
Basal area (m ² ha ⁻¹)	57.3	-	36.0	-	9.3	-
Canopy cover (%) [*]	85	-	80	-	27	-
Live canopy (%) ^{**}	89	-	37	-	100	-
CWD maximum height (cm)	30	-	49	-	60	-
Fuel load (kg ha ⁻¹)						
1 hr	19	-	95	-	151	-
10 hr	192	-	150	-	1589	-
100 hr	322	-	403	-	6038	-
1000 hr (sound)	4296	-	0	-	25477	-
1000 hr (rotten)	0	-	0	-	1268	-

473 *M* = mean; *SD* = standard deviation; dbh = diameter at breast height; CWD = coarse woody debris

474 (diameter > 7.6 cm); hr = hour

475 Fuel load size classes: $1 \text{ hr} \leq 0.6 \text{ cm}$, $0.6 \text{ cm} < 10 \text{ hr} \leq 2.5 \text{ cm}$, $2.5 \text{ cm} < 100 \text{ hr} \leq 7.6 \text{ cm}$, $1000 \text{ hr} > 7.6$
476 cm , volumes were calculated based on Brown (1974).

477 *Canopy cover (%) refers to the total percent canopy cover for a plot.

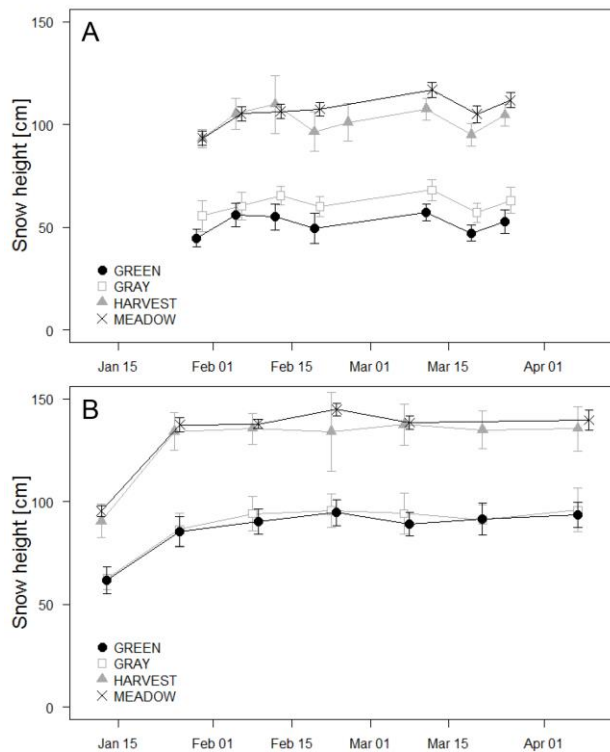
478 **Live canopy (%) refers to the percentage of canopy within a plot that is live (green).

479 **3.2 Snowpack characteristics and evolution**

480 *3.2.1 Snow height*

481 On average, snowpack was higher in winter of 2016 compared to 2015 (Fig. 4). Spatially
482 distributed snow depth measurements that were taken at every SMP sampling point during each
483 field campaign showed that HS for winter 2015 was highest in the MEADOW, followed by the
484 HARVEST, GRAY and GREEN plots (Fig. 5A). This pattern was found to be similar in winter of
485 2016 (Fig. 5B), although differences in HS between GREEN ($M = 87$, $SD = 12$) and GRAY ($M =$
486 89 , $SD = 14$) as well as between HARVEST ($M = 129$, $SD = 19$) and MEADOW ($M = 132$, $SD =$
487 17) plots were smaller compared to HS differences observed in the winter of 2015 (GREEN: $M =$
488 52 , $SD = 7$; GRAY: $M = 61$, $SD = 7$; HARVEST: $M = 102$, $SD = 10$; MEADOW: $M = 107$, $SD =$
489 8).

490



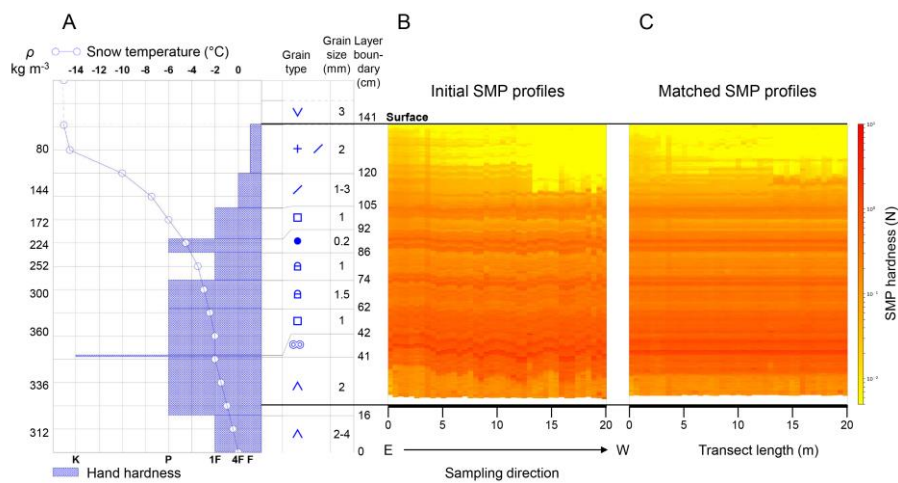
491
 492 **Fig. 5.** Evolution over time of the mean height of the snowpack (HS) measured along transects at
 493 GREEN, GRAY, HARVEST, and MEADOW study plots in A) 2015, N~34 per transect and date
 494 (Transects 1 to 8), and B) 2016, N~41 per transect and date (Transects 1 to 7, Table A1). Error bars
 495 represent standard deviations.

496 *3.2.2 Qualitative snowpack observations*

497 In general, larger differences in hardness that were measured by the SMP were also manually
 498 observed as layers of different hardness in the snow pit profiles excavated at the MEADOW plot.
 499 Figure 6 shows an example of a snow stratigraphy observed in the MEADOW plot on January
 500 25, 2016. For example, a hard snow layer was detected at 42 cm snow height by measurements
 501 from both the SMP and hand hardness tests in the snow pit. This continuous hard layer was
 502 correctly tracked by the matching algorithm and is visible in the snow hardness profile
 503 assembled from plotting SMP profiles side-by-side in the order they were taken along the

504 transect. Moreover, snow layers that were missed or misclassified by the snow pit observer can
505 be easily identified from the SMP derived snow hardness profile.

506



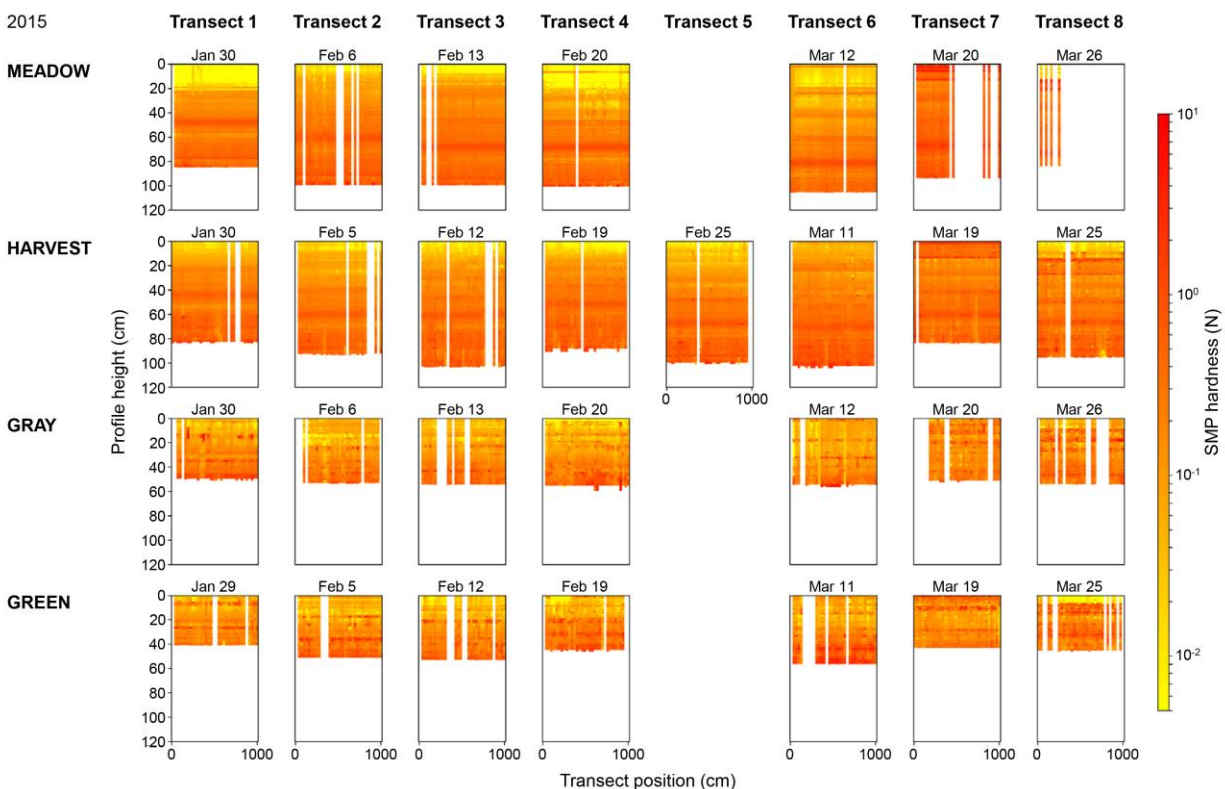
507

508 **Fig. 6.** Stratigraphy of the snowpack observed at the MEADOW plot on January 25, 2016: (A) in the
509 excavated snow pit profile, and, aligned to the corresponding height in the snow pit profile, (B and C)
510 along the sampled SMP transect (Transect 2, 2016). Initial (B) and matched (C) SMP profiles are plotted
511 side-by-side in the same order as measurements were taken in 0.5 m intervals. Visualization of snow pit
512 profile adapted from Snowpro Plus+ (snowprofile.ca). Symbols according to the International
513 Classification for Seasonal Snow (Fierz et al., 2009).

514 Throughout the winter of 2015, snow hardness profiles constructed from individual but
515 matched SMP profiles show that continuous persistent hard layers such as melt-freeze snow, and
516 wind or sun crusts were present in the MEADOW and HARVEST plots visible as dark red bands
517 in Figure 7. Distinct vertical and continuous slope-parallel hard and soft snow layers indicate that
518 snow stratigraphy is more homogeneous at these plots. In the GREEN and GRAY plots,
519 discontinuous hard and soft layers were observed at different snow heights within the snow

520 stratigraphy. These observations demonstrate a more heterogeneous snow stratigraphy
521 throughout the winter.

522



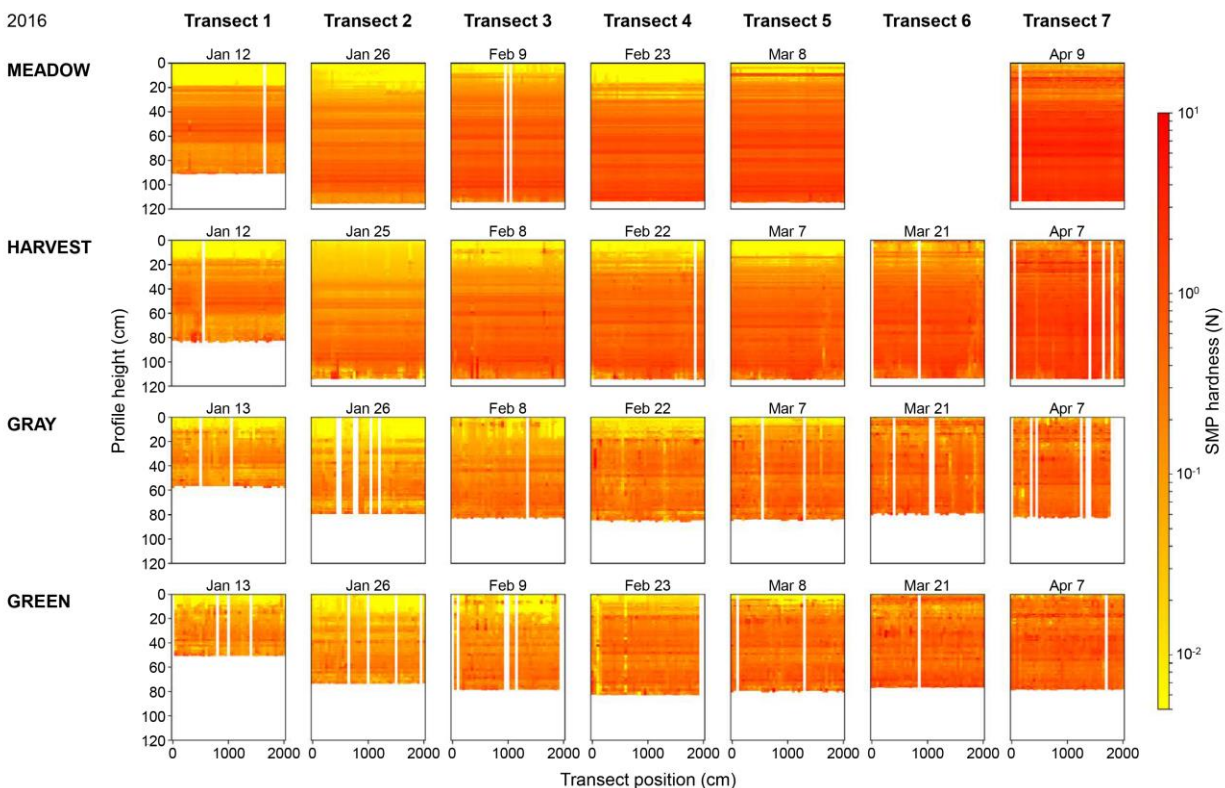
523

524 **Fig. 7.** Matched SMP profiles plotted side-by-side in the order taken in winter 2015 in the study plots
525 MEADOW, HARVEST, GRAY and GREEN every 0.3 m along 10 m long transects. Snow hardness
526 profile height corresponds to the actual snow height. Missing SMP profiles (white columns) are either
527 sampling points that were coinciding with a tree bole, or SMP profiles that were classified as > "C2"
528 according to the classification scheme of Pielmeier and Marshall (2009).

529 Similar results were observed throughout the winter of 2016, which, in contrast to the low
530 snowpack in 2015, was an average snowfall year (Figs. 4 and 5). However, an increase in
531 hardness with snow depth was more pronounced in the winter of 2016 in MEADOW and
532 HARVEST plots compared to winter 2015, and compared to GRAY and GREEN plots caused by

533 greater self-weight gravity snow settlement. At GREEN and GRAY plots, more homogeneous
 534 snow layers of different hardness were observed in the snowpack towards the end of the winter
 535 (Transects 5 to 7), but they were not as distinct during the beginning and the middle of the
 536 sampling period (Transect 1 to 4). Distinct and continuous hard layers, for example, buried sun,
 537 wind or melt-freeze crusts, and ice lenses (recorded as such in snow pit profiles) were present in
 538 the entire snowpack at HARVEST and MEADOW plots (Fig. 8).

539



540

541 **Fig. 8.** Matched SMP profiles plotted side-by-side in the order taken in winter 2016 in the study plots
 542 MEADOW, HARVEST, GRAY and GREEN every 0.5 m along 20 m long transects. Snow hardness
 543 profile height corresponds to the snow height that was present at GREEN and GRAY plots. Except for
 544 Transect 1, snow height exceeded the maximum SMP probe length of 1.2 m at MEADOW and
 545 HARVEST plots. Missing SMP profiles (white columns) are either sampling points that were coinciding

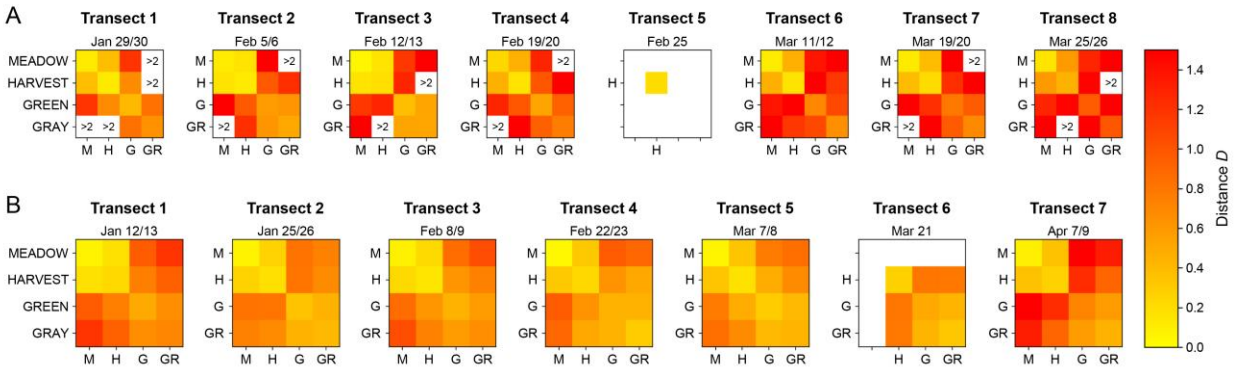
546 with a tree bole, or SMP profiles that were classified as > "C2" according to the classification scheme of
547 Pielmeier and Marshall (2009).

548 3.2.3 *Quantification of variability in snow stratigraphy*

549 In general, the computation of the similarity metric distance D revealed that SMP profiles
550 that are closer in space have lower D values than SMP profiles that are more distant, which
551 translates to a more similar snow stratigraphy from point to point (data not shown). Figure 9
552 shows a pair-wise comparison of the median D , that is, the median of all D for all matched SMP
553 profiles pairs collected at one day in the respective study plots. Two main groups are clearly
554 distinguishable: 1) the MEADOW and the HARVEST plots, and 2) the GREEN and the GRAY
555 plots. Median D retrieved by matching and comparing SMP profiles collected in a study plot of
556 one group with the SMP profiles from a study plot of the other group are clearly larger than D
557 within both groups. This is especially true for the winter of 2015 where numerous SMP profiles
558 collected in MEADOW and GRAY plots could not be matched for Transects 1, 2, 4, and 7 ($D >$
559 2) due to layer thickness variations that exceeded the set range of [-50%, +100%].

560 In contrast, median D within HARVEST and MEADOW, and between HARVEST and
561 MEADOW plots are small, which indicates a smaller slope-parallel variability in snow
562 stratigraphy and, therefore, a more homogeneous snow layering. Median D of GREEN and
563 GRAY plots as well as between GREEN and GRAY plots are larger pointing to a greater slope-
564 parallel variability, that is, a more heterogeneous snow stratigraphy.

565

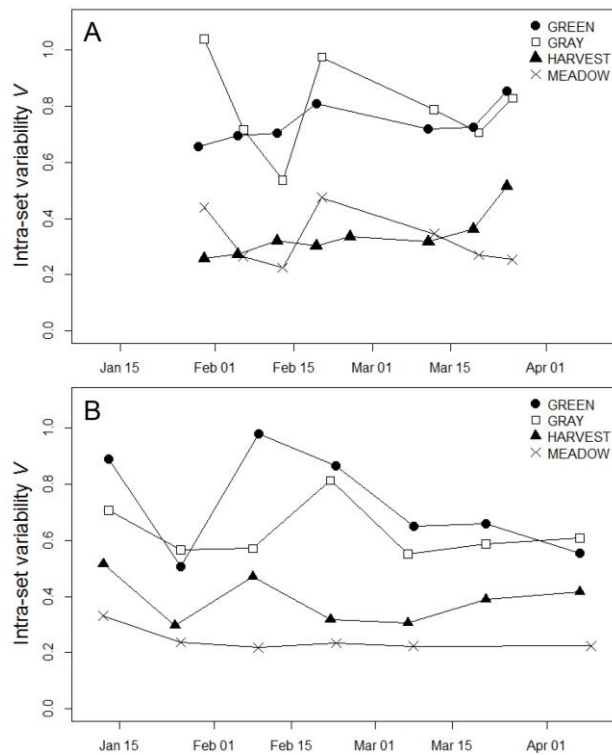


566

567 **Fig. 9.** Pair-wise comparison of the median of distance D computed from SMP profile pairs sampled
 568 along transects at GREEN (G), GRAY (GR), HARVEST (H), and MEADOW (M) study plots in A) 2015,
 569 and B) 2016.

570 This distinction between the two groups MEADOW/HARVEST and GREEN/GRAY is also
 571 visible in Figure 10, which shows the evolution of the intra-set variability V that was calculated
 572 for every transect collected at each of our four study plots. In both winters V , which quantifies
 573 how different the collected SMP profiles are, was found to be generally higher for transects
 574 sampled at GREEN/GRAY plots compared to MEADOW/HARVEST plots.

575



576

577 **Fig. 10.** Evolution over time of intra-set variability V calculated for transects sampled at GREEN, GRAY,
 578 HARVEST, and MEADOW study plots in A) 2015 (Transects 1 to 8), and B) 2016 (Transects 1 to 7,
 579 Table A1).

580 In 2016, values of V in the GREEN plot were mostly slightly higher than V -values calculated
 581 for the GRAY plot followed by HARVEST and MEADOW plots suggesting a decrease from a
 582 more heterogeneous to a more homogeneous snow stratigraphy in that order. For the latter one,
 583 we calculated the lowest V -values that changed only little over the course of the 2016 sampling
 584 period (Fig. 10B); however, greater fluctuations in V were found in 2015 (Fig. 10A). Values and
 585 range of V retrieved for the HARVEST plot were similar for both winters. Compared to 2016, V
 586 retrieved for transects collected at the GRAY plot in 2015 were higher with greater fluctuations
 587 over the sampling period (Fig. 10A). For the GREEN plot calculated V -values were found to be
 588 in a similar range in both years, but with greater fluctuations over the sampling period in 2016.

589 Repeated measures ANOVA and pairwise t-tests conducted with data combined for both
590 winters revealed no significant difference in V for GREEN ($M = 0.73$, $SD = 0.13$) and GRAY (M
591 $= 0.71$, $SD = 0.16$) plots; $t(14) = -0.14$, $p = 0.88$, and between HARVEST ($M = 0.36$, $SD = 0.08$)
592 and MEADOW ($M = 0.29$, $SD = 0.08$) plots; ($t(14) = -1.86$, $p = 0.08$). However, V differed
593 significantly between the two distinguished groups GREEN/GRAY ($M = 0.72$, $SD = 0.14$) and
594 MEADOW/HARVEST ($M = 0.33$, $SD = 0.09$) plots; ($t(27) = -13.25$, $p < 0.001$).

595 Based on the similar and, therefore, robust results from both metrics median D and V , the
596 above findings suggest that differences in the spatial variability in snow stratigraphy are related
597 to different canopy effects of green and gray stage spruce forest stands. In contrast, the canopy
598 cover of salvage-logged forests stands can be reduced to a degree where it has almost no effect
599 on the snowpack.

600 **3.3 Predictors of variability in snow stratigraphy**

601 Through model selection based on the AICc and F -tests we found that variations in V were
602 best explained by the percentage of canopy covering each transect observed on the SMP
603 sampling day according to the best-fit model containing data for both years. The percentage of
604 canopy cover was also the most important significant variable in combination with T_{a1} and $N1$
605 for 2015, and in combination with T_{a3} and $N3$ for 2016. Conditional R^2 -values for the best-fit
606 models range between 0.71 and 0.88 (Table 4). Two-way interactions of the chosen variables had
607 no significant effects on variations in V .

608

609 **Table 4**

610 Model formulas, AICc, marginal R^2 (R^2_m), and conditional R^2 (R^2_c) for the three best-fit models selected
611 for 2015, 2016, and for both years combined

Year	Model formula*	AICc	R ² _m	R ² _c
2015**	$V = f \{ \mathbf{CANOPY} + (1 \text{PLOT}) \}$	-70.9	0.61	0.71
and	$V = f \{ \mathbf{CANOPY} + \text{HS} + (1 \text{PLOT}) \}$	-70.4	0.63	0.71
2016	$V = f \{ \mathbf{CANOPY} + \text{HS} + \text{N3} + \text{T}_a\mathbf{1} + (1 \text{PLOT}) \}$	-70.0	0.65	0.73
2015	$V = f \{ \mathbf{CANOPY} + \mathbf{T}_a\mathbf{1} + \mathbf{N1} + (1 \text{PLOT}) \}$	-37.3	0.67	0.87
	$V = f \{ \mathbf{CANOPY} + \mathbf{T}_a\mathbf{1} + \text{N1} + \text{HS} + (1 \text{PLOT}) \}$	-36.5	0.69	0.88
	$V = f \{ \mathbf{CANOPY} + \mathbf{T}_a\mathbf{1} + \text{HS} + (1 \text{PLOT}) \}$	-36.2	0.71	0.85
2016	$V = f \{ \mathbf{CANOPY} + \mathbf{T}_a\mathbf{3} + \mathbf{N3} + (1 \text{PLOT}) \}$	-38.1	0.82	0.82
	$V = f \{ \mathbf{CANOPY} + (1 \text{PLOT}) \}$	-36.8	0.77	0.77
	$V = f \{ \mathbf{CANOPY} + \mathbf{T}_a\mathbf{1} + \Delta\text{T}_a\mathbf{3} + \mathbf{N3} + (1 \text{PLOT}) \}$	-35.6	0.82	0.82

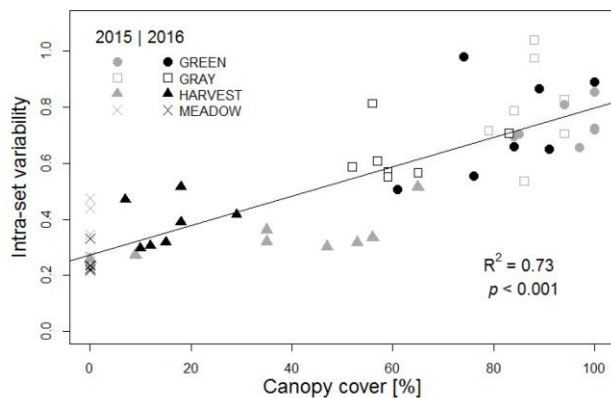
612 *Parameters in bold have significant coefficients ($p < 0.05$).

613 V = intra-set variability; **CANOPY** = percentage of canopy cover per transect; **HS** = mean height of the
614 snowpack; **N3** = accumulated precipitation 1 to 3 days prior to measurements; **T_a1** = average air
615 temperature 1 day prior to measurements; **N1** = accumulated precipitation 1 day prior to measurements;
616 **T_a3** = average air temperature within a 3-day period prior to measurements; $\Delta\text{T}_a\mathbf{3}$ = average air
617 temperature difference between 1 and 3 days prior to measurements; **PLOT** = plot categories GREEN,
618 GRAY, HARVEST and MEADOW; the parentheses indicate the term is a random effect (*re*), all other
619 terms are fixed effects; (1|*re*) indicates that the intercept was allowed to vary randomly. Parameters are
620 listed in order of importance.

621 **modelling YEAR as additional random effect (1|YEAR) did not enhance model fit.

622 Including the year sampled as random effect did not enhance the performance of the model
623 including data for both years. Therefore, we excluded “YEAR” and treated “PLOT” as the only
624 random effect for the models for both winters. The variance explained by the random effect
625 **PLOT**, which can be interpreted as the effect of the stage within the spruce bark beetle outbreak
626 cycle and its associated canopy condition GREEN, GRAY, HARVEST or MEADOW, ranged
627 between 0% in 2016 and 23% in 2015 (Table 4, calculated as fraction of the difference between

628 marginal R^2 and conditional R^2 of the conditional R^2). Since it was also only 14% for the best-fit
 629 model including both years' data, we, in addition, used linear regression to test for linear
 630 correlation between percentage of canopy cover and V . A highly significant positive correlation
 631 was found for both years' data (Fig. 11), but also between percentage of canopy cover and V that
 632 were observed in 2015 ($R^2 = 0.70$; $p < 0.001$), and in 2016 ($R^2 = 0.77$; $p < 0.001$). No linear
 633 correlations were found either between T_{a1} and V or between $N1$ and V (variables in the 2015
 634 best-fit LMM) as well as between T_{a3} and V or $N3$ and V (variables in the 2016 best-fit LMM).
 635



636
 637 **Fig. 11.** Intra-set variability V plotted against percentage of canopy cover for transects measured at
 638 GREEN, GRAY, HARVEST and MEADOW plots in 2015 and 2016. The R^2 and p -value are for the linear
 639 regression model that only includes percentage of canopy cover as explanatory variable. Regression line
 640 is shown for the significant linear relationship between canopy cover and V .

641 **4. Discussion**

642 **4.1 Effects of spruce bark beetle infestation on forest snowpack**

643 Our first hypothesis that, following spruce bark beetle infestation, the spatial variability in
 644 snow stratigraphy decreases gradually from a more heterogeneous snowpack to a more

645 homogeneous snowpack among non-infested to gray stage to salvage-logged spruce forest
646 stands, is not supported by our findings. The variability in snow stratigraphy (quantified by the
647 similarity metrics intra-set variability V and distance D) that we observed in winters of 2015 and
648 2016 over 10 and 20 m long transects, did not differ significantly between green and gray stage
649 Engelmann spruce forest stands. However, the snowpack in both stands was significantly more
650 heterogeneous compared to the snow stratigraphy that developed in salvage-logged and non-
651 forested areas. This heterogeneous layering of sub-canopy snowpack translates to disrupted and
652 discontinuous snow layers and weaknesses, and is the main reason why slab avalanche release
653 from dense healthy forest is inhibited (Gubler and Rychetnik, 1991; Schneebeli and Bebi, 2004;
654 Schneebeli and Meyer-Grass, 1993). We found that the percentage of canopy cover (out of all
655 tested forest and weather variables) was the main predictor that influenced the spatial variability
656 in subcanopy snow stratigraphy. Heterogeneity in snow stratigraphy increased with increasing
657 forest canopy cover. The method we used to determine the presence of canopy did not depend
658 solely on the presence of needles, but included additional canopy elements such as branches and
659 twigs. That is, the spatial variability in snow stratigraphy did not depend on only the reduction in
660 needle mass (i.e., the stage during the outbreak cycle) four to five years after the spruce beetle
661 infestation. In contrast, salvage logging that reduced the canopy cover to ~25%, led to a more
662 homogeneous snow stratigraphy. The snow stratigraphy found in this study plot was similar to
663 observations in the non-forested (meadow) plot where distinct and continuous slope-parallel soft
664 and hard snow layers including sun or wind crusts, ice lenses and weak layers (that we identified
665 as such in snow pit profiles) are generally more likely to form (Schweizer et al., 2003).

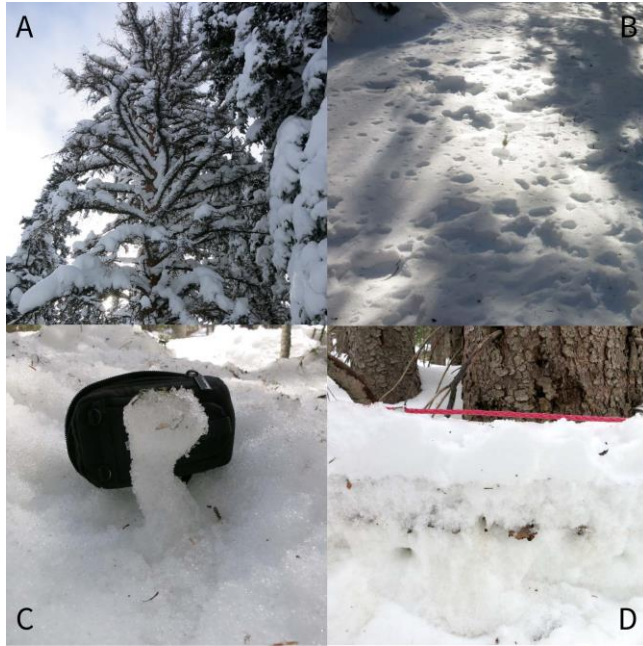
666 These differences in the spatial heterogeneity of snowpack properties between gray stage and
667 harvested areas was also found in a modeling study (Perrot et al., 2014); however, we did not

668 observe a clear decrease in the heterogeneity of the snowpack with the progression of foliage
669 loss (i.e., green to gray stage). This is especially true for the winter of 2015, which was
670 characterized by a below average snowpack and warm January and February mean air
671 temperatures. Compared to 2016, variability in snow stratigraphy of green and gray stage stands
672 was more similar despite the greater difference in the proportion of live canopy. Moreover,
673 differences between the two distinguished groups that had a similar variability in snow
674 stratigraphy (i.e., green/gray stage stand, and salvage-logged/non-forested area) were very
675 distinct. These differences were also found in 2016 but less pronounced suggesting the influence
676 of typical snow and meteorological patterns that were present in each year. Linear mixed models
677 that were fit to the data of each year separately revealed contributions of mean air temperature
678 and accumulated precipitation, but no significant linear relationship between either of those
679 variables and V was found.

680 We therefore examined air temperature and snow depth measurements (see Fig. 4) that were
681 present prior to field campaigns where greater differences in V between green and gray stage
682 stands were found (see Fig. 10). Three campaigns stand out: January 29/20 (Transect 1) and
683 February 19/20 (Transect 4) in 2015, and February 8/9 (Transect 3) in 2016. In January 2015,
684 mean air temperatures were above 0°C and no new snow had fallen in the study region since the
685 middle of the month. We therefore assume that more melt-freeze snow may have been formed in
686 locations in less shaded areas along the transect in the gray stage stand compared to the green
687 stand, which could have led to a greater spatial variability in snow stratigraphy. In the gray
688 stand's snow hardness profile, a discontinuous harder layer close to the snow surface can be
689 identified, but also small areas of very hard snow at a depth of 10 cm (Fig. 7). According to our
690 field notes and in field observations, these areas could be ice clumps that were a result of

691 refrozen melt water dripping from the canopy into the snowpack (Fig. 12C). The same process
692 could have also influenced the greater variability in snow stratigraphy observed in the gray stage
693 stand in February of the same year. Prior to that campaign, little snow had fallen, and air
694 temperatures had increased suggesting that snow intercepted by dead trees melted faster
695 compared to snow that was intercepted in live canopies. Meltwater dripping from branches forms
696 meltwater channels in the snowpack which, after refreezing, are assumed to interrupt continuous
697 snow layers with low tensile strength and to have a stabilizing effect on the snowpack (Gubler
698 and Rychetnik, 1991). Schweizer et al. (1995) performed snowpack stability tests below the area
699 projected by the crowns of larch trees and found that such a snowpack has greater tensile
700 strength compared to areas just outside the projected crown area. The snowpack stabilizing effect
701 of canopy drip is therefore restricted to the projected crown (Bründl et al., 1999). However, in
702 contrast to the parts of protection forests at the upper tree line that mainly consist of larch with
703 tree distances often exceeding 15 m, gray stage spruce stands still remain the physical structure
704 of the original dense forest. Therefore, the snowpack stabilizing effect of increased canopy drip
705 below crowns of larch trees is also present in gray stage spruce stands and even more
706 pronounced because of the usually higher stem and canopy densities.

707



708

709 **Fig. 12.** Processes influencing subcanopy snow stratigraphy in forests after spruce beetle infestation: A)
 710 Snow intercepted by crowns of dead (gray) Engelmann spruce; B) Depressions at the snow surface
 711 created by unloading or melting of intercepted snow; C) Melt water that dripped from branches created
 712 melt channels in the snowpack and, after refreezing, emerged at the snow surface during snowmelt; D)
 713 Bark flakes that accumulated around woodpecker-debarked trunks of beetle-infested trees got
 714 subsequently buried in the snowpack. Photos: Michaela Teich

715 Beginning of February 2016, mean air temperatures were very low ($\sim -15^{\circ}\text{C}$) and snow fall
 716 was reported during this cold period prior to our data collection, but mean air temperatures had
 717 increased to $\sim -5^{\circ}\text{C}$ at the time of sampling (we measured 1°C in the afternoon at the study site).
 718 The amount of snow initially intercepted by a crown depends on branch structure and is
 719 influenced by wind, temperature, and solar radiation during deposition (Sturm, 1992). Therefore,
 720 this combination of cold temperatures and snow fall could have reduced snow interception by
 721 dead tree crowns while more snow may have been intercepted in the green stand that unloaded as
 722 relatively dense snow clumps with increasing air temperatures (Hedstrom and Pomeroy, 1998;

723 Schmidt and Pomeroy, 1990). These effects of green versus gray canopy interacting with low
724 temperatures during snowfall followed by an increase in temperature could have resulted in the
725 observed greater spatial variability in snow stratigraphy in the green compared to the gray stage
726 stand. For example, Pfister and Schneebeli (1999) showed how temperature influences the
727 interception efficiency on wooden boards of different sizes and shapes, which can be interpreted
728 as differences between green and gray stage spruce forest stands. Because adhesion of snow to
729 twigs increases as temperature rises toward the freezing point, differences between live and dead
730 trees may be more important when temperature during snowfall is low. In addition to the
731 influence of the canopy coverage itself, these interactions could have also led to the greater
732 differences in snow depth measured on February 8/9, 2016 between the gray stage stand ($M = 94$
733 cm) and the green stand ($M = 90$ cm) as well as on March 7/8 that year (green: $M = 94$ cm; gray:
734 $M = 88$ cm). The snowfall prior to our measurements in early-March 2016 was accompanied by a
735 decrease in air temperature (see Fig. 4), although differences in the variability in snow
736 stratigraphy were rather low.

737 Our second hypothesis is, therefore, not fully supported by our findings. Forest canopy
738 condition was not found to be the main predictor for changes to the spatial variability in snow
739 stratigraphy. Even with the majority of foliage absent from the canopy of gray stage spruce
740 forests, the standing dead snags still affect snow stratigraphy similarly to green forest stands. We
741 attribute this to the small fine branches and twigs still present in the canopy influencing snow
742 interception, snow unloading and canopy drip (Fig. 12), and moderating wind and solar
743 radiation. However, canopy related processes, which contribute to a higher or lower snowpack
744 heterogeneity may differ under specific meteorological conditions as well as on different slope
745 aspects and angles. Therefore, future long-term studies that in particular include winters with

746 well above average snow fall are needed to further investigate the protective capacity of gray
747 stage avalanche protection forests. In addition, influences on snow stratigraphy due to energy
748 balances associated with varying slope angles and aspects coupled with forest canopy loss
749 requires further investigation.

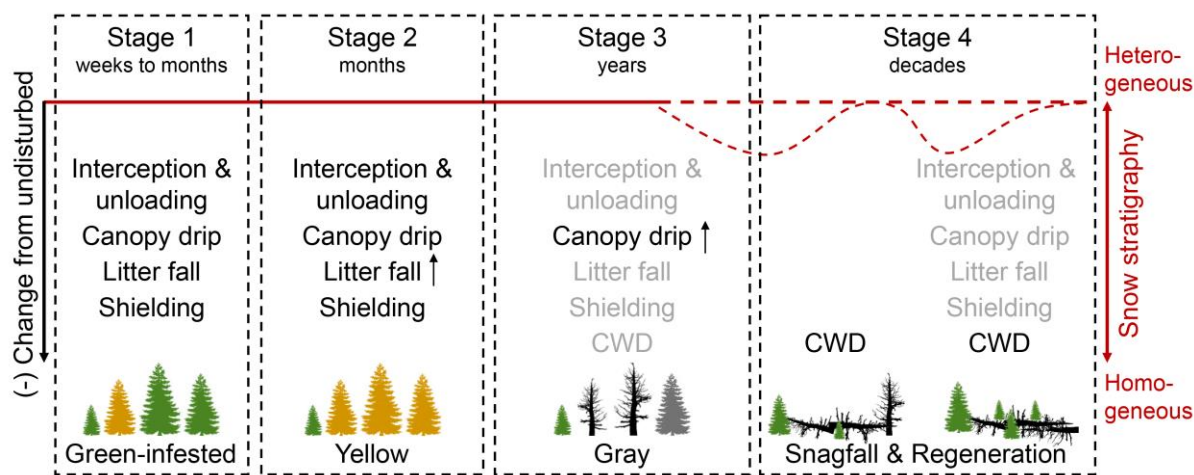
750 Our third hypothesis that surface roughness in terms of the amount and height of CWD is
751 linked to snowpack heterogeneity was not supported by our findings. We measured the highest
752 volume of sound CWD at our salvage logged plot compared to the other forested plots, but the
753 snow stratigraphy was found to be homogeneous and similar to a non-forested area. However,
754 although surface roughness was increased through remaining logging slash, this slash was
755 mainly composed of FWD fuel classes, which can be easily buried during the initial early season
756 snow fall. The sound CWD was mostly comprised of pieces of tree limbs and branches, and the
757 majority of large CWD pieces such as tree boles were removed from this stand. The maximum
758 height of CWD was fairly consistent among the three forested plot types, but only few dead and
759 down tree boles were present mainly in the gray stage stand. Therefore, increasing roughness by
760 leaving wood in a gray stand after salvage logging may only help to disrupt continuous layers
761 and weaknesses in the snowpack, if large stems and/or high stumps and root plates are kept in the
762 stand (McClung, 2001).

763 **4.2 Potential impacts on avalanche formation**

764 Based on our findings and personal observations while revisiting the study plots every week
765 or every other week over two consecutive winter seasons, we conclude that spruce forest stands
766 up to at least five years after the initial infestation are capable of providing adequate protection
767 against avalanche formation and release. The processes of the canopy interacting with certain
768 snow and weather conditions may differ between the different stages during a spruce bark beetle

769 outbreak cycle but lead to the same result: a heterogeneous snow stratigraphy that is less prone to
 770 avalanche release. In Figure 13 and below, we summarize the most important processes for each
 771 stage during a spruce bark beetle outbreak cycle and discuss implications for avalanche
 772 protection forest management after spruce bark beetle infestation.

773



774

775 **Fig. 13.** Conceptual model of avalanche formation following spruce bark beetle outbreak for the stages 1)
 776 green-infested (current year's attack), 2) yellow (previous year's attack), 3) gray (approximately three to
 777 five years post infestation), and 4) snagfall and regeneration. Processes that do not change compared to
 778 undisturbed forests are shown in black. Processes that decrease in importance relative to undisturbed
 779 forests are shown in gray. Arrows indicate an increase relative to non-infested stands. Depending on the
 780 rate of snagfall between Stages 3 and 4, the probability for avalanche formation may decrease temporarily
 781 (especially during periods of heavy snow fall accompanied by cold air temperatures). The same is true, if
 782 decay rates of logs are faster than the establishment of sufficiently advanced regeneration. See Section 4.2
 783 for further descriptions.

784 Stage 1 – Green-infested (current year's attack): Dense and mature spruce forest stands
 785 without canopy gaps wider than 20 m provide avalanche protection through canopy interception

786 and subsequent unloading of intercepted snow (Bebi et al., 2009; Schneebeli and Meyer-Grass,
787 1993). Snow clumps dumping from branches embedded in the snowpack as well as meltwater
788 dripping into the snowpack below canopies disrupt the snow stratigraphy and, therefore, prevent
789 the formation of continuous snow layers and weaknesses, which is the prerequisite for avalanche
790 formation in forests (Bründl et al., 1999; Schweizer et al., 2003). The wind shielding effect of
791 forests reduces snow redistribution and compaction, and therefore the formation of a fine slope-
792 parallel layering and hard- or wind-compacted snow slabs (Gubler and Rychetnik, 1991). Wind
793 speed reduction and shading of the snowpack by the canopy also change the energy balance at
794 the snow surface leading to more moderate temperature fluctuations, which reduces the
795 formation of weak layers (Schneebeli and Bebi, 2004).

796 Stage 2 - Yellow (previous year's attack): In general, the same processes as in green-infested
797 stands apply. In addition, needle release begins and debarking of infested trees by woodpeckers
798 may occur, depositing needles and bark flakes onto the snow surface, which are subsequently
799 buried in the snowpack throughout the snow season (Fig. 12D). The increase in the amount of
800 organic material modifies the albedo and the radiation regime at the snow surface (Pugh and
801 Gordon, 2013; Winkler et al., 2010), and creates flow channels for dripping meltwater (Bründl et
802 al., 1999). Because needles and bark flakes have a lower albedo than snow they absorb more heat
803 and emit long-wave radiation, which creates little melt depressions acting as entry ways for
804 preferential flow. A layer of organic material buried in the snowpack can create an uneven
805 boundary between snow layers, which also favors preferential flow of meltwater in the
806 snowpack. Dripping meltwater, vertical flow and refreezing in the snowpack prevent the
807 formation of weak layers and increase the stability of the snowpack.

808 Stage 3 - Gray (approximately three to five years post-infestation): At the beginning of this
809 stage (at least up to five years after infestation), small branches and twigs that remain in the
810 canopy as well as falling needles and branches provide similar protective benefits as green,
811 green-infested and yellow stands. Although snow interception might be reduced during snow fall
812 with air temperatures well below freezing level (Pfister and Schneebeli, 1999), unloading and an
813 increase in canopy drip and preferential flow result in a similar heterogeneous snow stratigraphy
814 as found in green, green-infested and yellow stands (Bründl et al., 1999). The stabilizing effect of
815 gray trees may even exceed the snowpack stability found beneath larch crowns (Schweizer et al.,
816 1995), since spruce stands are usually higher in density. Once small branches start to release and
817 the canopy structure starts to breakup through the loss of bigger branches and limbs, an increase
818 in homogeneity in snow stratigraphy is expected to reach its maximum as the canopy is no longer
819 shading the snowpack, and canopy drip is significantly reduced.

820 Stage 4 – Snagfall and regeneration (decades after initial infestation): Once snagfall occurs,
821 snow stratigraphy may gradually become more heterogeneous again as large diameter tree boles
822 contribute to discontinuous snow layers, if the remaining standing and downed woody debris are
823 spatially distributed without gaps larger than 20 m (Schönenberger et al., 2005; Feistl et al.,
824 2014). It was found that areas in avalanche protection forests that were disturbed by wind and
825 not cleared after the event occurred, effectively prevented avalanche release for at least ten and
826 up to 20 years following the disturbance (Frey and Thee, 2002; Wohlgemuth et al., 2017). In
827 contrast to windthrow, which occurs during one single event, snagfall in forests following spruce
828 bark beetle disturbance is often more gradual, but such stands are also prone to additional wind
829 disturbance. Kupferschmid Albisetti et al. (2003) found that 75% of snags in a Norway spruce
830 mountain forest that was killed by European spruce bark beetle were already broken four to eight

831 years after infestation caused by a storm event and increased wind speeds. They concluded that
832 leaving such stands unharvested is likely to result in effective protection against avalanche
833 release for about 30 years after infestation. The protective effect of woody debris will
834 increasingly be replaced by future regeneration once seedlings and saplings are twice as high as
835 the expected maximum snow height, and forest succession moves from stem initiation to stem-
836 exclusion and closed-canopy stages. However, a critical “protection gap period” with reduced
837 overall protection against natural hazards as suggested against rockfall after wind disturbance
838 may occur (Frey and Thee, 2002), if snagfall and decay rates of logs are faster than the
839 establishment of sufficiently advanced regeneration. In addition, the establishment of new
840 seedlings and saplings on decaying Norway spruce logs may be hindered by the presence of
841 brown-rot-causing fungus *Fomitopsis pinicola* (Fr.) Karst. in European spruce bark beetle killed
842 forests (Bače et al., 2012).

843 **4.3 Implications for avalanche protection forest management**

844 Following spruce bark beetle infestation, it is common practice to implement some form of
845 salvage logging or sanitation felling to reduce localized beetle population pressure and the
846 buildup of hazardous fuels, and to recoup some economic value from infested trees (Collins et
847 al., 2012; Jenkins et al., 2014; Stadelmann et al., 2013). In Norway spruce forests of the
848 European Alps, reducing the spread of a European spruce bark beetle infestation within and into
849 adjacent stands can be critical to prevent the extent of an outbreak throughout an avalanche
850 protection forest (Stadelmann et al., 2014). When spruce bark beetle populations have reached
851 epidemic phases, decisions about optimal management strategies (within a reasonable time and
852 at reasonable costs) become thus more challenging.

853 For such forest areas where the maintenance of the protective effect is the highest priority,
854 our results suggest that it is often more appropriate to leave dead trees in place. Results from our
855 salvage-logged study plot, which had a lower stem density and, more importantly, a lower
856 overall canopy cover, show that the snow stratigraphy that developed at this plot was
857 homogeneous and similar to the stratigraphy found in the adjacent un-forested meadow. This
858 indicates an insufficient protective effect in harvested stands where the majority of overstory
859 large diameter trees was removed, which is comparable to clear-cut areas (McClung, 2001). On a
860 larger spatial scale, removing infested and dead trees can affect local wind regimes resulting in
861 higher wind speeds, which can increase snow drift and compaction, and loading of slopes that
862 were previously shielded by forests (Teich et al., 2016). Consequently, post-outbreak harvest
863 management decisions can greatly influence the future snow stratigraphy and thus avalanche
864 formation.

865 We recognize that in areas where the European spruce bark beetle pressure is endemic,
866 management activities such as removal of infested trees through sanitation felling, and individual
867 and small group salvage logging would be appropriate. These areas include, for example,
868 important designated protection forest stands, recreation areas such as ski resorts, and viewsheds
869 that are important for tourism to limit the loss and impact on these resources from future beetle
870 infestations. Although, removing infested trees can be difficult and costly (e.g., by helicopter-
871 assisted logging operations) due to the often limited accessibility to the terrain.

872 Strategies to increase resistance (decreased susceptibility) and resilience to a spruce bark
873 beetle infestation, demand to manipulate stand structure and species composition (Brang, 2001;
874 Jenkins et al., 2014; Motta and Haudemand, 2000; Schmid and Frye, 1977; Temperli et al.,
875 2014). In order to decrease the susceptibility to infestations and to foster advanced regeneration,

876 forest managers could supplement regeneration cuts with planting to increase species diversity
877 and the proportion of non-host species (Wohlgemuth et al., 2017). This would also create more
878 structural diversity, that is, uneven and multi-layered stands with a mosaic of tree sizes and age
879 classes, which are ideal for long-term avalanche protection (e.g., Bachofen and Zingg, 2001; Ott
880 et al., 1997; Motta and Haudemand, 2000). Following spruce bark beetle outbreak, it may be
881 necessary to help accelerate forest succession in avalanche prone areas while also increasing
882 future species diversity by local planting (Wohlgemuth et al., 2017). In high-risk areas where
883 protective effects of the remaining gray stage stand and additional planting are still not
884 considered to be sufficient, additional protection measures against avalanche formation and snow
885 drift (e.g., wooden snow fences and tripods) may be required.

886 In addition to sanitation felling and planting, forest managers must consider how to manage
887 the CWD load following spruce bark beetle infestation. Although our findings did not support
888 our hypothesis that increased CWD as observed in the salvage-logged forest stand would lead to
889 a more heterogeneous snow stratigraphy, the majority of the present CWD were not tree boles.
890 Moreover, our gray stage stand had yet to reach the snagfall stage and almost all dead trees
891 remained standing. It has been found that retaining fallen trees after wind disturbance in Norway
892 spruce dominated avalanche and rock fall protection forests still provides protective capacity
893 through increased surface roughness (Schönenberger et al., 2005; Wohlgemuth et al., 2017).
894 Moreover, these studies were conducted in wind disturbed forests where the predominant
895 direction of snagfall is related to the wind direction in contrast to spruce bark beetle killed stands
896 without subsequent wind disturbance. This approach is easier and less expensive than active
897 management, and often maintains adequate protection against avalanches (Kulakowski et al.,
898 2017; Kupferschmid Albisetti et al., 2003). Additionally, in cases where only groups of trees are

899 infested as in an endemic phase, individual trees could be felled and debarked to prevent further
900 spread of spruce bark beetles (Jenkins et al., 2014), and left in place as a snowpack stabilizing
901 element. In order to further improve the protective effect by CWD, it may be necessary to
902 strategically orient (i.e., 30 to 45° to the slope direction) and anchor these logs, and to
903 periodically check their position, anchoring and decay rate (BAFU, 2008).

904 **4.4 Conclusions**

905 With climate change, more frequent and severe bark beetle outbreaks are expected. Mountain
906 forests, which often serve an important role in avalanche protection are therefore prone to
907 drastically increasing disturbances by spruce bark beetle, with uncertain consequences for the
908 avalanche hazard.

909 Our findings from studying the temporal and spatial variability of snow stratigraphy in non-
910 infested, gray stage and salvage-logged Engelmann spruce forest stands show that snow
911 stratigraphy under canopies of non-infested and gray stage stands is similar and generally more
912 heterogeneous compared to salvage-logged forests and non-forested areas. The small fine
913 branches and twigs that are still present in the canopy five years after the initial attack maintain
914 snow interception and unloading, and especially increase canopy drip. However, such canopy
915 related processes that stabilize the snowpack may be reduced during specific meteorological
916 conditions, that is, during extended periods of snowfall accompanied by cold air temperatures
917 and in winters with above average snowfall. Salvage logging that reduced the canopy cover to
918 ~25%, led to a homogeneous snow stratigraphy similar to the layering found in non-forested
919 areas, which is prone to avalanche formation. Residual logging slash did not increase the surface
920 roughness enough to affect the snow stratigraphy; however, increased surface roughness after
921 snagfall is a more effective protection measure.

922 Thus, our study suggests to leave dead trees and downed woody material in place, especially
923 in protection forests where bark beetle populations have reached epidemic phases. Additionally,
924 in cases where only groups of trees are infested as in an endemic phase, felling and debarking
925 individual trees and anchoring of large debarked logs can prevent further spread of spruce bark
926 beetles and stabilize the snowpack. Overall, logging operations and silvicultural measures after
927 bark beetle disturbance in forests with a protective function have to be planned and carried out
928 carefully. To provide sustainable long-term protection against avalanches, forest management
929 decisions in spruce dominated forests must focus on increasing structural and species diversities
930 and thus resilience to mitigate the severity of future attacks.

931 Future long-term studies are needed to address questions of how long and under what
932 meteorological conditions the protective effect of gray stage stands will be sufficient as canopy
933 structure declines with time since the initial outbreak.

934 **Acknowledgments**

935 We thank the USDA Forest Service's Intermountain Region-Forest Health Protection group
936 Ogden, UT personnel and especially Darren Blackford and Liz Hebertson for their help with
937 field work and site selection. We are grateful to Ted Scroggin and Mark Nelson from the USDA
938 Forest Service Evanston Ranger District Uinta-Wasatch-Cache National Forest for providing
939 logistical support in the field. We also thank Curtis Gray and Sarah Null for field assistance as
940 well as the anonymous reviewer for their helpful comments to an earlier version of the
941 manuscript. This work was supported by the USU Department of Wildland Resources; the USDA
942 Forest Service; and the Swiss National Science Foundation [grant numbers P2EZIP2_155606,
943 P300P2_171236].

944 **References**

- 945 Akaike, H., 1973. Information Theory and an Extension of the Maximum Likelihood Principle, in: Petrov,
946 B.N., Csaki, F. (Eds.), Second International Symposium on Information Theory. Akademiai Kiado,
947 Budapest, pp. 267–281.
- 948 Bače, R., Svoboda, M., Pouska, V., Janda, P., Červenka, J., 2012. Natural regeneration in Central-
949 European subalpine spruce forests: Which logs are suitable for seedling recruitment? *For. Ecol.*
950 *Manage.* 266, 254–262. <https://doi.org/10.1016/j.foreco.2011.11.025>
- 951 Bachofen, H., Zingg, A., 2001. Effectiveness of structure improvement thinning on stand structure in
952 subalpine Norway spruce (*Picea abies* (L.) Karst.) stands. *For. Ecol. Manage.* 145, 137–149.
953 [https://doi.org/10.1016/S0378-1127\(00\)00581-8](https://doi.org/10.1016/S0378-1127(00)00581-8)
- 954 BAFU, 2008. Sturmschaden-Handbuch. Vollzugshilfe für die Bewältigung von Sturmschadenereignissen
955 von nationaler Bedeutung im Wald. Umwelt-Vollzug Nr. 0801., 3. überarb. ed. Bundesamt für
956 Umwelt, Bern.
- 957 Baier, P., Pennerstorfer, J., Schopf, A., 2007. PHENIPS—A comprehensive phenology model of *Ips*
958 *typographus* (L.) (Col., Scolytinae) as a tool for hazard rating of bark beetle infestation. *For. Ecol.*
959 *Manage.* 249, 171–186. <https://doi.org/10.1016/j.foreco.2007.05.020>
- 960 Barton, K., 2018. MuMIn: Multi-Model Inference, R package version 1.40.4. < [https://cran.r-](https://cran.r-project.org/package=MuMIn)
961 [project.org/package=MuMIn](https://cran.r-project.org/package=MuMIn)>.
- 962 Bates, D., Mächler, M., Bolker, B., Walker, S., 2015. Fitting Linear Mixed-Effects Models Using lme4. *J.*
963 *Stat. Softw.* 67, 1–48. <https://doi.org/10.18637/jss.v067.i01>
- 964 Bebi, P., Kulakowski, D., Rixen, C., 2009. Snow avalanche disturbances in forest ecosystems—State of
965 research and implications for management. *For. Ecol. Manage.* 257, 1883–1892.
966 <https://doi.org/10.1016/j.foreco.2009.01.050>
- 967 Bebi, P., Seidl, R., Motta, R., Fuhr, M., Firm, D., Krumm, F., Conedera, M., Ginzler, C., Wohlgemuth, T.,
968 Kulakowski, D., 2017. Changes of forest cover and disturbance regimes in the mountain forests of
969 the Alps. *For. Ecol. Manage.* 388, 43–56. <https://doi.org/10.1016/j.foreco.2016.10.028>
- 970 Bentz, B.J., Duncan, J.P., Powell, J.A., 2016. Elevational shifts in thermal suitability for mountain pine
971 beetle population growth in a changing climate. *Forestry* 89, 271–283.
972 <https://doi.org/10.1093/forestry/cpv054>
- 973 Bentz, B.J., Régnière, J., Fettig, C.J., Hansen, E.M., Hayes, J.L., Hicke, J.A., Kelsey, R.G., Negrón, J.F.,

974 Seybold, S.J., 2010. Climate Change and Bark Beetles of the Western United States and Canada:
975 Direct and Indirect Effects. *Bioscience* 60, 602–613. <https://doi.org/10.1525/bio.2010.60.8.6>

976 Biederman, J.A., Brooks, P.D., Harpold, A.A., Gochis, D.J., Gutmann, E., Reed, D.E., Pendall, E., Ewers,
977 B.E., 2014. Multiscale observations of snow accumulation and peak snowpack following
978 widespread, insect-induced lodgepole pine mortality. *Ecohydrology* 7, 150–162.
979 <https://doi.org/10.1002/eco.1342>

980 Black, S.H., Kulakowski, D., Noon, B.R., DellaSala, D.A., 2013. Do Bark Beetle Outbreaks Increase
981 Wildfire Risks in the Central U.S. Rocky Mountains? Implications from Recent Research. *Nat.*
982 *Areas J.* 33, 59–65. <https://doi.org/10.3375/043.033.0107>

983 Boon, S., 2009. Snow ablation energy balance in a dead forest stand. *Hydrol. Process.* 23, 2600–2610.
984 <https://doi.org/10.1002/hyp.7246>

985 Brang, P., 2001. Resistance and elasticity: promising concepts for the management of protection forests in
986 the European Alps. *For. Ecol. Manage.* 145, 107–119. [https://doi.org/10.1016/S0378-
987 1127\(00\)00578-8](https://doi.org/10.1016/S0378-1127(00)00578-8)

988 Brang, P., Schönenberger, W., Frehner, M., Schwitter, R., Thormann, J.J., Wasser, B., 2006. Management
989 of protection forests in the European Alps: An overview. *For. Snow Landsc. Res.* 80, 23–44.

990 Brown, J.K., 1974. Handbook for Inventorying Downed Woody Material, USDA For. Serv. Gen. Tech.
991 Rep. INT-16. U.S. Department of Agriculture, Forest Service, Intermountain Forest and Range
992 Experiment Station, Ogden, UT.

993 Bründl, M., Schneebeli, M., Flühler, H., 1999. Routing of canopy drip in the snowpack below a spruce
994 crown. *Hydrol. Process.* 13, 49–58. [https://doi.org/10.1002/\(SICI\)1099-1085\(199901\)13:1<49::AID-
995 HYP700>3.0.CO;2-L](https://doi.org/10.1002/(SICI)1099-1085(199901)13:1<49::AID-HYP700>3.0.CO;2-L)

996 Collins, B.J., Rhoades, C.C., Battaglia, M.A., Hubbard, R.M., 2012. The effects of bark beetle outbreaks
997 on forest development, fuel loads and potential fire behavior in salvage logged and untreated
998 lodgepole pine forests. *For. Ecol. Manage.* 284, 260–268.
999 <https://doi.org/10.1016/j.foreco.2012.07.027>

1000 Coulson, R.N., 1979. Population Dynamics of Bark Beetles. *Annu. Rev. Entomol.* 24, 417–447.
1001 <https://doi.org/10.1146/annurev.en.24.010179.002221>

1002 DeRose, R.J., Long, J.N., 2009. Wildfire and spruce beetle outbreak: Simulation of interacting
1003 disturbances in the central Rocky Mountains. *Écoscience* 16, 28–38. [https://doi.org/10.2980/16-1-
1004 3160](https://doi.org/10.2980/16-1-3160)

1005 Dorren, L.K.A., Berger, F., Imeson, A.C., Maier, B., Rey, F., 2004. Integrity, stability and management of
1006 protection forests in the European Alps. *For. Ecol. Manage.* 195, 165–176.
1007 <https://doi.org/10.1016/j.foreco.2004.02.057>

1008 Edburg, S.L., Hicke, J.A., Brooks, P.D., Pendall, E.G., Ewers, B.E., Norton, U., Gochis, D., Gutmann,
1009 E.D., Meddens, A.J.H., 2012. Cascading impacts of bark beetle-caused tree mortality on coupled
1010 biogeophysical and biogeochemical processes. *Front. Ecol. Environ.* 10, 416–424.
1011 <https://doi.org/10.1890/110173>

1012 Faccoli, M., 2009. Effect of Weather on *Ips typographus* (Coleoptera Curculionidae) Phenology,
1013 Voltinism, and Associated Spruce Mortality in the Southeastern Alps. *Environ. Entomol.* 38, 307–
1014 316. <https://doi.org/10.1603/022.038.0202>

1015 Faccoli, M., Bernardinelli, I., 2014. Composition and Elevation of Spruce Forests Affect Susceptibility to
1016 Bark Beetle Attacks: Implications for Forest Management. *Forests* 5, 88–102.
1017 <https://doi.org/10.3390/f5010088>

1018 Feistl, T., Bebi, P., Dreier, L., Hanewinkel, M., Bartelt, P., 2014. Quantification of basal friction for
1019 technical and silvicultural glide-snow avalanche mitigation measures. *Nat. Hazards Earth Syst. Sci.*
1020 14, 2921–231. <https://doi.org/10.5194/nhess-14-2921-2014>

1021 Fettig, C.J., Klepzig, K.D., Billings, R.F., Munson, A.S., Nebeker, T.E., Negrón, J.F., Nowak, J.T., 2007.
1022 The effectiveness of vegetation management practices for prevention and control of bark beetle
1023 infestations in coniferous forests of the western and southern United States. *For. Ecol. Manage.* 238,
1024 24–53. <https://doi.org/10.1016/j.foreco.2006.10.011>

1025 Fiebigler, G., 1978. Ursachen von Waldlawinen im Bereich der nordöstlichen Randalpen und ihre
1026 Behandlung durch forsttechnische Massnahmen. Dissertation, Universität für Bodenkultur Wien.

1027 Fierz, C., Armstrong, R.L., Durand, Y., Etchevers, P., Greene, E., McClung, D.M., Nishimura, K.,
1028 Satyawali, P.K., Sokratov, S.A., 2009. The international classification for seasonal snow on the
1029 ground. Vol. 25. Paris: UNESCO/IHP.

1030 Fox, J., Weisberg, S., 2011. An {R} Companion to Applied Regression, Second Edition. Sage, Thousand
1031 Oaks CA.

1032 Frey, W., Thee, P., 2002. Avalanche protection of windthrow areas: A ten year comparison of cleared and
1033 uncleared starting zones. *For. Snow Landsc. Res.* 77, 89–107.

1034 Gillies, R.R., Wang, S.-Y., Booth, M.R., 2012. Observational and Synoptic Analyses of the Winter
1035 Precipitation Regime Change over Utah. *J. Clim.* 25, 4679–4698. <https://doi.org/10.1175/JCLI-D->

- 1036 11-00084.1
- 1037 Grodzki, W., 2008. Spatio-temporal patterns of the Norway spruce decline in the Beskid Śląski and
1038 Żywiecki (Western Carpathians) in southern Poland. *J. For. Sci.* 53, 38–44.
1039 <https://doi.org/10.17221/2155-JFS>
- 1040 Gubler, H., Rychetnik, J., 1991. Effects of forests near the timberline on avalanche formation, in:
1041 Bergmann, H. et al. (Ed.), *Snow, Hydrology and Forests in High Alpine Areas*, Proceedings of the
1042 Vienna Symposium, August 1991, IAHS Publications 205. Vienna, Austria, pp. 19–37.
- 1043 Hagemuller, P., Pilloix, T., 2016. A New Method for Comparing and Matching Snow Profiles,
1044 Application for Profiles Measured by Penetrometers. *Front. Earth Sci.* 4, 1–13.
1045 <https://doi.org/10.3389/feart.2016.00052>
- 1046 Harrison, X.A., Donaldson, L., Correa-Cano, M.E., Evans, J., Fisher, D.N., Goodwin, C.E.D., Robinson,
1047 B.S., Hodgson, D.J., Inger, R., 2018. A brief introduction to mixed effects modelling and multi-
1048 model inference in ecology. *PeerJ* 6, e4794. <https://doi.org/10.7717/peerj.4794>
- 1049 Hebertson, E.G., Jenkins, M.J., 2007. The Influence of Fallen Tree Timing on Spruce Beetle Brood
1050 Production. *West. North Am. Nat.* 67, 452–460. [https://doi.org/10.3398/1527-](https://doi.org/10.3398/1527-0904(2007)67[452:TIOFTT]2.0.CO;2)
1051 [0904\(2007\)67\[452:TIOFTT\]2.0.CO;2](https://doi.org/10.3398/1527-0904(2007)67[452:TIOFTT]2.0.CO;2)
- 1052 Hedstrom, N.R., Pomeroy, J.W., 1998. Measurements and modelling of snow interception in the boreal
1053 forest. *Hydrol. Process.* 12, 1611–1625. [https://doi.org/10.1002/\(SICI\)1099-](https://doi.org/10.1002/(SICI)1099-1085(199808/09)12:10/11<1611::AID-HYP684>3.0.CO;2-4)
1054 [1085\(199808/09\)12:10/11<1611::AID-HYP684>3.0.CO;2-4](https://doi.org/10.1002/(SICI)1099-1085(199808/09)12:10/11<1611::AID-HYP684>3.0.CO;2-4)
- 1055 Hurvich, C.M., Tsai, C.-L., 1989. Regression and time series model selection in small samples.
1056 *Biometrika* 76, 297–307. <https://doi.org/10.1093/biomet/76.2.297>
- 1057 Imbeck, H., 1983. Schneeuntersuchungen in subalpinen Fichtenwäldern. *Schweizerische Zeitschrift für*
1058 *Forstwes.* 134, 925–928.
- 1059 Imbeck, H., Ott, E., 1987. Verjüngungsökologische Untersuchungen in einem hochstaudenreichen
1060 subalpinen Fichtenwald, mit spezieller Berücksichtigung der Schneeablagerung und der
1061 Lawinenbildung. *Mitteilungen des Eidgenössischen Institutes für Schnee- und Lawinenforsch.* 42,
1062 202 pp.
- 1063 Jenkins, M., Hebertson, E., Munson, A., 2014. Spruce Beetle Biology, Ecology and Management in the
1064 Rocky Mountains: An Addendum to Spruce Beetle in the Rockies. *Forests* 5, 21–71.
1065 <https://doi.org/10.3390/f5010021>
- 1066 Jenkins, M.J., Hebertson, E., Page, W., Jorgensen, C.A., 2008. Bark beetles, fuels, fires and implications

1067 for forest management in the Intermountain West. *For. Ecol. Manage.* 254, 16–34.
1068 <https://doi.org/10.1016/j.foreco.2007.09.045>

1069 Jenkins, M.J., Page, W.G., Hebertson, E.G., Alexander, M.E., 2012. Fuels and fire behavior dynamics in
1070 bark beetle-attacked forests in Western North America and implications for fire management. *For.*
1071 *Ecol. Manage.* 275, 23–34. <https://doi.org/10.1016/j.foreco.2012.02.036>

1072 Johnson, J.B., Schneebeli, M., 1999. Characterizing the microstructural and micromechanical properties
1073 of snow. *Cold Reg. Sci. Technol.* 30, 91–100. [https://doi.org/10.1016/S0165-232X\(99\)00013-0](https://doi.org/10.1016/S0165-232X(99)00013-0)

1074 Jonášová, M., Prach, K., 2008. The influence of bark beetles outbreak vs. salvage logging on ground layer
1075 vegetation in Central European mountain spruce forests. *Biol. Conserv.* 141, 1525–1535.
1076 <https://doi.org/10.1016/j.biocon.2008.03.013>

1077 Jönsson, A.M., Appelberg, G., Harding, S., Barring, L., 2009. Spatio-temporal impact of climate change
1078 on the activity and voltinism of the spruce bark beetle, *Ips typographus*. *Glob. Chang. Biol.* 15, 486–
1079 499. <https://doi.org/10.1111/j.1365-2486.2008.01742.x>

1080 Jorgensen, C.A., Jenkins, M.J., 2011. Fuel Complex Alterations Associated with Spruce Beetle-Induced
1081 Tree Mortality in Intermountain Spruce/Fir Forests. *For. Sci.* 57, 232–240.
1082 <https://doi.org/10.1093/forestscience/57.3.232>

1083 Kronholm, K., Schneebeli, M., Schweizer, J., 2004. Spatial variability of micropenetration resistance in
1084 snow layers on a small slope. *Ann. Glaciol.* 38, 202–208.
1085 <https://doi.org/10.3189/172756404781815257>

1086 Kulakowski, D., Seidl, R., Holeksa, J., Kuuluvainen, T., Nagel, T.A., Panayotov, M., Svoboda, M., Thorn,
1087 S., Vacchiano, G., Whitlock, C., Wohlgemuth, T., Bebi, P., 2017. A walk on the wild side:
1088 Disturbance dynamics and the conservation and management of European mountain forest
1089 ecosystems. *For. Ecol. Manage.* 388, 120–131. <https://doi.org/10.1016/j.foreco.2016.07.037>

1090 Kupferschmid Albisetti, A.D., Brang, P., Schönenberger, W., Bugmann, H., 2003. Decay of *Picea abies*
1091 snag stands on steep mountain slopes. *For. Chron.* 79, 247–252. <https://doi.org/10.5558/tfc79247-2>

1092 Lindenmayer, D.B., Noss, R.F., 2006. Salvage Logging, Ecosystem Processes, and Biodiversity
1093 Conservation. *Conserv. Biol.* 20, 949–958. <https://doi.org/10.1111/j.1523-1739.2006.00497.x>

1094 Logan, J.A., Macfarlane, W.W., Willcox, L., 2010. Whitebark pine vulnerability to climate-driven
1095 mountain pine beetle disturbance in the Greater Yellowstone Ecosystem. *Ecol. Appl.* 20, 895–902.
1096 <https://doi.org/10.1890/09-0655.1>

1097 Marshall, H.-P., Johnson, J.B., 2009. Accurate inversion of high-resolution snow penetrometer signals for

- 1098 microstructural and micromechanical properties. *J. Geophys. Res.* 114, F04016.
1099 <https://doi.org/10.1029/2009JF001269>
- 1100 McClung, D.M., 2001. Characteristics of terrain, snow supply and forest cover for avalanche initiation
1101 caused by logging. *Ann. Glaciol.* 32, 223–229. <https://doi.org/10.3189/172756401781819391>
- 1102 Molotch, N.P., Barnard, D.M., Burns, S.P., Painter, T.H., 2016. Measuring spatiotemporal variation in
1103 snow optical grain size under a subalpine forest canopy using contact spectroscopy. *Water Resour.*
1104 *Res.* 52, 7513–7522. <https://doi.org/10.1002/2016WR018954>
- 1105 Motta, R., Haudemand, J.-C., 2000. Protective Forests and Silvicultural Stability. *Mt. Res. Dev.* 20, 180–
1106 187. [https://doi.org/10.1659/0276-4741\(2000\)020\[0180:PFASS\]2.0.CO;2](https://doi.org/10.1659/0276-4741(2000)020[0180:PFASS]2.0.CO;2)
- 1107 Müller, J., Bußler, H., Goßner, M., Rettelbach, T., Duelli, P., 2008. The European spruce bark beetle *Ips*
1108 *typographus* in a national park: from pest to keystone species. *Biodivers. Conserv.* 17, 2979–3001.
1109 <https://doi.org/10.1007/s10531-008-9409-1>
- 1110 Munroe, J.S., 2003. Holocene timberline and palaeoclimate of the northern Uinta Mountains, northeastern
1111 Utah, USA. *The Holocene* 13, 175–185. <https://doi.org/10.1191/0959683603hl600rp>
- 1112 Nakagawa, S., Schielzeth, H., 2013. A general and simple method for obtaining R^2 from generalized
1113 linear mixed-effects models. *Methods Ecol. Evol.* 4, 133–142. [https://doi.org/10.1111/j.2041-](https://doi.org/10.1111/j.2041-210x.2012.00261.x)
1114 [210x.2012.00261.x](https://doi.org/10.1111/j.2041-210x.2012.00261.x)
- 1115 Olschewski, R., Bebi, P., Teich, M., Wissen Hayek, U., Grêt-Regamey, A., 2012. Avalanche protection by
1116 forests — A choice experiment in the Swiss Alps. *For. Policy Econ.* 15, 108–113.
1117 <https://doi.org/10.1016/j.forpol.2011.10.002>
- 1118 Ott, E., Frehner, M., Frey, H., Lüscher, P., 1997. *Gebirgsnadelwälder. Ein praxisorientierter Leitfaden für*
1119 *eine standortsgerechte Waldbehandlung.* Paul Haupt, Bern, Stuttgart, Wien.
- 1120 Page, W.G., Jenkins, M.J., Runyon, J.B., 2014. Spruce Beetle-Induced Changes to Engelmann Spruce
1121 Foliage Flammability. *For. Sci.* 60, 691–702. <https://doi.org/10.5849/forsci.13-050>
- 1122 Perrot, D., Molotch, N.P., Musselman, K.N., Pugh, E.T., 2014. Modelling the effects of the mountain pine
1123 beetle on snowmelt in a subalpine forest. *Ecohydrology* 7, 226–241.
1124 <https://doi.org/10.1002/eco.1329>
- 1125 Petitjean, F., Ketterlin, A., Gançarski, P., 2011. A global averaging method for dynamic time warping,
1126 with applications to clustering. *Pattern Recognit.* 44, 678–693.
1127 <https://doi.org/10.1016/j.patcog.2010.09.013>

- 1128 Pfister, R., Schneebeli, M., 1999. Snow accumulation on boards of different sizes and shapes. *Hydrol.*
1129 *Process.* 13, 2345–2355. [https://doi.org/10.1002/\(SICI\)1099-1085\(199910\)13:14/15<2345::AID-](https://doi.org/10.1002/(SICI)1099-1085(199910)13:14/15<2345::AID-)
1130 [HYP873>3.0.CO;2-N](https://doi.org/10.1002/(SICI)1099-1085(199910)13:14/15<2345::AID-HYP873>3.0.CO;2-N)
- 1131 Pielmeier, C., Marshall, H.-P., 2009. Rutschblock-scale snowpack stability derived from multiple quality-
1132 controlled SnowMicroPen measurements. *Cold Reg. Sci. Technol.* 59, 178–184.
1133 <https://doi.org/10.1016/j.coldregions.2009.06.005>
- 1134 Pielmeier, C., Schneebeli, M., 2003. Stratigraphy and changes in hardness of snow measured by hand,
1135 ramsonde and snow micro penetrometer: a comparison with planar sections. *Cold Reg. Sci. Technol.*
1136 37, 393–405. [https://doi.org/10.1016/S0165-232X\(03\)00079-X](https://doi.org/10.1016/S0165-232X(03)00079-X)
- 1137 Pinzer, B.R., Schneebeli, M., Kaempfer, T.U., 2012. Vapor flux and recrystallization during dry snow
1138 metamorphism under a steady temperature gradient as observed by time-lapse micro-tomography.
1139 *Cryosph.* 6, 1141–1155. <https://doi.org/10.5194/tc-6-1141-2012>
- 1140 Pugh, E., Gordon, E., 2013. A conceptual model of water yield effects from beetle-induced tree death in
1141 snow-dominated lodgepole pine forests. *Hydrol. Process.* 27, 2048–2060.
1142 <https://doi.org/10.1002/hyp.9312>
- 1143 Pugh, E., Small, E., 2012. The impact of pine beetle infestation on snow accumulation and melt in the
1144 headwaters of the Colorado River. *Ecohydrology* 5, 467–477. <https://doi.org/10.1002/eco.239>
- 1145 Pugh, E.T., Small, E.E., 2013. The impact of beetle-induced conifer death on stand-scale canopy snow
1146 interception. *Hydrol. Res.* 44, 644–657. <https://doi.org/10.2166/nh.2013.097>
- 1147 R Core Team, 2018. R: A language and environment for statistical computing. Vienna, Austria.
1148 [<http://www.R-project.org/>](http://www.R-project.org/).
- 1149 Raffa, K.F., Aukema, B.H., Bentz, B.J., Carroll, A.L., Hicke, J.A., Turner, M.G., Romme, W.H., 2008.
1150 Cross-scale Drivers of Natural Disturbances Prone to Anthropogenic Amplification: The Dynamics
1151 of Bark Beetle Eruptions. *Bioscience* 58, 501–517. <https://doi.org/10.1641/B580607>
- 1152 Reuter, B., Richter, B., Schweizer, J., 2016. Snow instability patterns at the scale of a small basin. *J.*
1153 *Geophys. Res. Earth Surf.* 121, 257–282. <https://doi.org/10.1002/2015JF003700>
- 1154 Schmid, J.M., Frye, R.H., 1977. Spruce Beetle in the Rockies, USDA Forest Service General Technical
1155 Report. U.S. Department of Agriculture, Fort Collins, CO.
- 1156 Schmidt, R.A., Pomeroy, J.W., 1990. Bending of a conifer branch at subfreezing temperatures:
1157 implications for snow interception. *Can. J. For. Res.* 20, 1251–1253. <https://doi.org/10.1139/x90-165>

- 1158 Schneebeli, M., Bebi, P., 2004. Snow and Avalanche Control. *Encycl. For. Sci.* 397–402.
- 1159 Schneebeli, M., Johnson, J.B., 1998. A constant-speed penetrometer for high-resolution snow stratigraphy.
1160 *Ann. Glaciol.* 26, 107–111. <https://doi.org/10.3189/1998AoG26-1-107-111>
- 1161 Schneebeli, M., Meyer-Grass, M., 1993. Avalanche starting zones below the timber line—structure of
1162 forest, in: *Proceedings of the International Snow Science Workshop, 4-8 October 1992.*
1163 Breckenridge, CO, pp. 176–181.
- 1164 Schönenberger, W., Noack, A., Thee, P., 2005. Effect of timber removal from windthrow slopes on the
1165 risk of snow avalanches and rockfall. *For. Ecol. Manage.* 213, 197–208.
1166 <https://doi.org/10.1016/j.foreco.2005.03.062>
- 1167 Schweizer, J., Jamieson, J.B., Schneebeli, M., 2003. Snow avalanche formation. *Rev. Geophys.* 41, 1016.
1168 <https://doi.org/10.1029/2002RG000123>
- 1169 Schweizer, J., Schneebeli, M., Fierz, C., Föhn, P.M.B., 1995. Snow mechanics and avalanche formation:
1170 field experiments on the dynamic response of the snow cover. *Surv. Geophys.* 16, 621–633.
1171 <https://doi.org/10.1007/BF00665743>
- 1172 Seidl, R., Schelhaas, M.-J., Lindner, M., Lexer, M.J., 2009. Modelling bark beetle disturbances in a large
1173 scale forest scenario model to assess climate change impacts and evaluate adaptive management
1174 strategies. *Reg. Environ. Chang.* 9, 101–119. <https://doi.org/10.1007/s10113-008-0068-2>
- 1175 Seidl, R., Schelhaas, M.-J., Rammer, W., Verkerk, P.J., 2014. Increasing forest disturbances in Europe and
1176 their impact on carbon storage. *Nat. Clim. Chang.* 4, 806–810. <https://doi.org/10.1038/nclimate2318>
- 1177 Shaw, J.D., Long, J.N., 2007. Forest Ecology and Biogeography of the Uinta Mountains, U.S.A. Arctic,
1178 Antarctic. *Alp. Res.* 39, 614–628. [https://doi.org/10.1657/1523-0430\(06-046\)\[SHAW\]2.0.CO;2](https://doi.org/10.1657/1523-0430(06-046)[SHAW]2.0.CO;2)
- 1179 Stadelmann, G., Bugmann, H., Meier, F., Wermelinger, B., Bigler, C., 2013. Effects of salvage logging
1180 and sanitation felling on bark beetle (*Ips typographus* L.) infestations. *For. Ecol. Manage.* 305, 273–
1181 281. <https://doi.org/10.1016/j.foreco.2013.06.003>
- 1182 Stadelmann, G., Bugmann, H., Wermelinger, B., Bigler, C., 2014. Spatial interactions between storm
1183 damage and subsequent infestations by the European spruce bark beetle. *For. Ecol. Manage.* 318,
1184 167–174. <https://doi.org/10.1016/j.foreco.2014.01.022>
- 1185 Sturm, M., 1992. Snow distribution and heat flow in the taiga. *Arct. Alp. Res.* 24, 145–152.
1186 <https://doi.org/10.1080/00040851.1992.12002939>
- 1187 Sturm, M., Benson, C., 2004. Scales of spatial heterogeneity for perennial and seasonal snow layers. *Ann.*

- 1188 Glaciol. 38, 253–260. <https://doi.org/10.3189/172756404781815112>
- 1189 Teich, M., Marty, C., Gollut, C., Grêt-Regamey, A., Bebi, P., 2012. Snow and weather conditions
1190 associated with avalanche releases in forests: Rare situations with decreasing trends during the last
1191 41years. *Cold Reg. Sci. Technol.* 83–84, 77–88. <https://doi.org/10.1016/j.coldregions.2012.06.007>
- 1192 Teich, M., Schneebeli, M., Bebi, P., Giunta, A.D., Gray, C.A., Jenkins, M.J., 2016. Effects of bark beetle
1193 attacks on snowpack and snow avalanche hazard, in: *Proceedings of the International Snow Science*
1194 *Workshop, 3-7 October 2016. Breckenridge, CO, pp. 975–983.*
- 1195 Teich, M., Techel, F., Caviezel, P., Bebi, P., 2013. Forecasting forest avalanches : A review of winter
1196 2011/12, in: *Proceedings of the International Snow Science Workshop, 7-11 October 2013. Grenoble*
1197 *– Chamonix Mont-Blanc, France, pp. 324–330.*
- 1198 Temperli, C., Hart, S.J., Veblen, T.T., Kulakowski, D., Hicks, J.J., Andrus, R., 2014. Are density reduction
1199 treatments effective at managing for resistance or resilience to spruce beetle disturbance in the
1200 southern Rocky Mountains? *For. Ecol. Manage.* 334, 53–63.
1201 <https://doi.org/10.1016/j.foreco.2014.08.028>
- 1202 Veblen, T.T., Hadley, K.S., Reid, M.S., Rebertus, A.J., 1991. The Response of Subalpine Forests to Spruce
1203 Beetle Outbreak in Colorado. *Ecology* 72, 213–231. <https://doi.org/10.2307/1938916>
- 1204 Winkler, R., Boon, S., Zimonick, B., Baleshta, K., 2010. Assessing the effects of post-pine beetle forest
1205 litter on snow albedo. *Hydrol. Process.* 24, 803–812. <https://doi.org/10.1002/hyp.7648>
- 1206 Winkler, R., Boon, S., Zimonick, B., Spittlehouse, D., 2014. Snow accumulation and ablation response to
1207 changes in forest structure and snow surface albedo after attack by mountain pine beetle. *Hydrol.*
1208 *Process.* 28, 197–209. <https://doi.org/10.1002/hyp.9574>
- 1209 Wohlgemuth, T., Schwitter, R., Bebi, P., Sutter, F., Brang, P., 2017. Post-windthrow management in
1210 protection forests of the Swiss Alps. *Eur. J. For. Res.* 136, 1029–1040.
1211 <https://doi.org/10.1007/s10342-017-1031-x>
- 1212 Xu, R., 2003. Measuring explained variation in linear mixed effects models. *Stat. Med.* 22, 3527–3541.
1213 <https://doi.org/10.1002/sim.1572>
- 1214 Zingg, T., 1958. Beitrag zur Untersuchung der Schneedecke im Walde am Beispiel Laret-Davos, Interner
1215 Bericht Nr. 289. Eidg. Institut für Schnee- und Lawinenforschung, Weissfluhjoch-Davos.
- 1216 Zuur, A.F., Ieno, E.N., Walker, N.J., Saveliev, A.A., Smith, G.M., 2009. *Mixed effects models and*
1217 *extensions in ecology with R.* Spring Science and Business Media, New York, NY.

1218 **Appendix**

1219 **Table A1**

1220 Sampling dates for Transects 1 to 8 in 2015 and Transects 1 to 7 in 2016 at four study plots GREEN,

1221 GRAY, HARVEST, and MEADOW at the study site in the Uinta Mountains in Utah, USA.

Sampling date and plot					
Transect no.	Year	GREEN	GRAY	HARVEST	MEADOW
Transect 1	2015	January 29	January 30	January 30	January 30
Transect 2		February 5	February 6	February 5	February 6
Transect 3		February 12	February 13	February 12	February 13
Transect 4		February 19	February 20	February 19	February 20
Transect 5		NA	NA	February 25	NA
Transect 6		March 11	March 12	March 11	March 12
Transect 7		March 19	March 20	March 19	March 20
Transect 8		March 25	March 26	March 25	March 26
Transect 1	2016	January 13	January 13	January 12	January 12
Transect 2		January 26	January 26	January 25	January 26
Transect 3		February 9	February 8	February 8	February 9
Transect 4		February 23	February 22	February 22	February 23
Transect 5		March 8	March 7	March 7	March 8
Transect 6		March 21	March 21	March 21	NA
Transect 7		April 7	April 7	April 7	April 9

1222